Cretaceous Research 102 (2019) 37–58

Contents lists available at ScienceDirect

Cretaceous Research

journal homepage: www.elsevier.com/locate/CretRes

A giant elasmosaurid (Sauropterygia; Plesiosauria) from Antarctica: New information on elasmosaurid body size diversity and aristonectine evolutionary scenarios

J.P. O'Gorman [a, b, *], S. Santillana [c], R. Otero [d, e], M. Reguero [a, c]

[a] División Paleontología Vertebrados, Museo de La Plata, Universidad Nacional de La Plata, Paseo del Bosque s/n., B1900FWA, La Plata, Argentina
[b] CONICET: Consejo Nacional de Investigaciones Científicas y Técnicas, Argentina, Godoy Cruz 2290, C1425FQB, CABA, Argentina
[c] instituto Antartico Argentino, 25 de Mayo 1143, B1650HMK, San Martín, Buenos Aires, Argentina
[d] Red Paleontológica U-Chile, Laboratorio de Ontogenia y Filogenia, Departamento de Biología, Facultad de Ciencias, Universidad de Chile, Las Palmeras, 3425, Santiago, Chile
[e] Consultora Paleosuchus Ltda. Huelén 165, Oficina C, Providencia, Santiago, Chile

ARTICLE INFO

Article history:
Received 21 May 2018
Received in revised form
12 April 2019
Accepted in revised form 10 May 2019
Available online 17 May 2019

Keywords:
Elasmosauridae
Aristonectinae
Aristonectes
López de Bertodano
Upper cretaceous

ABSTRACT

Aristonectines show a highly derived morphology among elasmosaurid plesiosaurs, including some species with large body size. A new postcranial skeleton is described from the uppermost Maastrichtian levels of the López de Bertodano Formation, Seymour Island (= *Marambio*), Antarctica, being referred to as cf. *Aristonectes* sp; the most striking feature of the specimen described is its large body size, among the largest elasmosaurids worldwide. The occurrence of this specimen, located approximately 2.3 m or less below the Cretaceous-Paleogene (K/Pg) boundary, indicates the persistence of aristonectines at high latitudes and also it verifies their chronostratigraphical distribution until the end Cretaceous, before the mass extinction. Elasmosaurid diversity in terms of body size, possible relation of this body size, the trophic niche and abiotic drivers in aristonectine evolution are discussed. The body size inferred for MLP 89-III-3-1 seems to indicate an environment with high primary productivity, suggesting that these conditions persisted until the K/Pg mass extinction.

1. Introduction

Elasmosaurids form a clade of long-necked plesiosaurs that radiated globally during the Late Cretaceous (Carpenter, 1999; Vincent et al., 2011; O'Gorman, 2016a; Serratos et al., 2017; Sachs et al., 2018). This worldwide abundance is also recorded along the Weddellian Province (i.e. Patagonia, Western Antarctica and New Zealand; Zinsmeister, 1979; Cruickshank and Fordyce, 2002; Gasparini et al., 2003; O'Gorman, 2012; O'Gorman et al., 2013a, b, 2015; Otero et al., 2014a, c; Hiller et al., 2017). Despite this widespread record and the large number of available specimens, elasmosaurids have been mostly considered as an extremely conservative clade, with variation centred in the relative neck length (O'Keefe and Hiller, 2006).

Among Late Cretaceous elasmosaurids, a distinctive group, the Aristonectinae (i.e. *Aristonectes* spp., *Kaiwhekea katiki*, *Morturneria seymourensis*, *Alexandronectes zealandiensis*) shows the acquisition of a secondary relatively less elongated neck compared to other elasmosaurids, due the combined reduction in the number of cervical vertebrae and shortening of cervical centra. Additionally, aristonectines show a highly derived number of relatively gracile teeth in skull and mandible (Chatterjee and Small, 1989; Cruickshank and Fordyce, 2002; Gasparini et al., 2003; Otero et al., 2014c; O'Keefe et al., 2017). Some of these features, particularly, the tooth number and cervical centrum proportions, were acquired convergently by cryptoclidid plesiosaurs, leading to challenging interpretations during the second half of the 20th century regarding the survival of the latter clade until the Late Cretaceous (Cabrera, 1941; Welles, 1952, 1962; Cruickshank and Fordyce, 2002; O'Keefe and Street, 2009). However, modern large-scale phylogenetic analyses (Gasparini

* Corresponding author. División Paleontología Vertebrados, Museo de La Plata, Universidad Nacional de La Plata, Paseo del Bosque s/n., B1900FWA, La Plata, Argentina.
E-mail addresses: joseogorman@fcnym.unlp.edu.ar (J.P. O'Gorman), ssantillana@dna.gov.ar (S. Santillana), otero2112@gmail.com (R. Otero), mreguero@dna.gov.ar (M. Reguero).

https://doi.org/10.1016/j.cretres.2019.05.004
0195-6671/

et al., 2003; Ketchum and Benson, 2010; Otero et al., 2012; O'Gorman, 2016a; Sachs and Kear, 2017; Sachs et al., 2017, 2018) have reached a consensus regarding the elasmosaurid affinities of aristonectines.

A recent result on aristonectine systematics and morphology has greatly improved our knowledge. The description of *Aristonectes quiriquinensis* (Otero et al., 2014b) showed that within the genus *Aristonectes* at least two different species were present in the Pacific and the Atlantic margins during the end of the Cretaceous (*A. quiriquinensis* and *A. parvidens*, respectively). An additional species, *Morturneria seymourensis* is known only based on a juvenile specimen from Seymour Island (=Marambio), Antarctica, and has been recently re-described (O'Keefe et al., 2017). The other species currently considered an aristonectine, *Alexandronectes zealandiensis*, seems to be a basal, relatively medium-size aristonectine; however this assumption is only based on its skull (Otero et al., 2016). The biogeographic background of the known species within the genus *Aristonectes*, both restricted to the upper Maastrichtian, naturally raises questions about the specific identity of contemporary aristonectine specimens from Antarctica. Additionally, aristonectines have been the main issue of recent discussion related to their trophic niche and the interpretation of their highly derived morphology (O'Gorman, 2016b; O'Keefe et al., 2017; Otero et al., 2018). Thus any new specimen increases knowledge and allows testing of previous hypotheses. During the 1989–1990 Antarctic Fieldwork, Dr. W.J. Zinsmeister (Purdue University) found a postcranial skeleton in the uppermost Maastrichtian levels (approximately 2.3 m meters or less below the K/Pg limit) of the López de Bertodano Formation, Seymour Island (=Marambio) (Zinsmeister et al., 1989; Crame et al., 2004, Fig. 1). Subsequently, the specimen was collected during four Antarctic campaigns by the authors and J.J. Moly (Museo de La Plata) during the Summer Antarctic Fieldtrips of the Instituto Antártico Argentino (IAA). Previous to this description, the specimen was briefly commented by O'Gorman et al. (2014), who described the gastrolith set associated with it. Also, its femur was included in the comparison of Weddellian elasmosaurids, for assessing the diagnostic value of the hemispherical head of the former genus '*Mauisaurus*' (Otero et al., 2015), currently considered as *nomen dubium* (Hiller et al., 2017).

The main aim of this study is to describe this postcranial skeleton, discussing its affinities with other aristonectines, as well as the implication of its body size, trophic niche and the presence of a large body-sized elasmosaurid near the K/Pg boundary in Antarctica.

1.1. Institutional abbreviations

AMNH, American Museum of Natural History, New York, USA; **ANSP**, Academy of Natural Sciences of Philadelphia, USA; **CD**, Chordata collection, National Paleontological Collection, GNS Science, Lower Hutt, New Zealand; **CM**, Canterbury Museum, Christchurch, New Zealand; **DM**, Museum of New Zealand Te Papa Tongarewa, Wellington, New Zealand; **DMNH**, Denver Museum Natural History, Colorado, USA; **LACM**, Natural History Museum of Los Angeles County, Los Angeles County, USA (previously housed in the **CIT**, California Institute of Technology, Pasadena, California); **MCS**, Museo de Cinco Saltos, Rio Negro Province, Argentina; **MLP**, Museo de la Plata, La Plata, Argentina; **NSM**, National Museum of Nature and Science, Tokyo, Japan; **OU**, Geology Museum, University of Otago, Dunedin, New Zealand; **SGO.PV**, Paleontología de Vertebrados, Museo Nacional de Historia Natural, Santiago, Chile; **TMP**, Tyrrell Museum of Palaeontology, Drumheller, Alberta, Canada; **UCMP**, University of California Paleontological Museum, San Francisco, USA.

1.2. Anatomical abbreviations

ao, accessory ossification; **azy**, anterior zygapophyses; **cap**, capitulum; **car**, caudal rib; **cf**, coracoid facet; **cr**, cervical rib; **css**, coracoids symphyseal surface; **dc**, distal carpal; **dlp**, dorsolateral process; **ep**, epipodial foramen; **f**, fibula, **fi**, fibulare; **gf**, glenoid facet; **gr**, glenoid ramus; **h**, humerus; **hf**, hemal facets; **in**, intermedium; **mc**, metacarpal; **ms**, muscle scar; **na**, neural arch; **nc**, neural canal; **pa**, parapophysis; **ph**, phalanx; **r**, radius; **ra**, radiale; **t**, tibia; **ti**, tibiale; **tp**, transverse process; **tr**, trochanter; **tu**, tuberosity; **u**, ulna; **ul**, ulnare; **vf**, ventral foramen; **vn**, ventral notch; **vr**, ventral ramus.

2. Geological setting

The Upper Cretaceous succession of the James Ross Archipelago is grouped into the upper Coniacian–Danian Marambio Group (Macellari, 1988; McArthur et al., 2000; Olivero and Medina, 2000, Crame et al., 2004, Olivero et al., 2008). The López Bertodano Formation, one of the better studied and thicker formations of the James Ross Archipelago, consists of sandstones and claystones interbedded with hard calcareous levels (Macellari, 1988). The formation is divided into nine informal units (named Klb 2 to Klb10, following Macellari, 1988 and Olivero et al., 2008) (Fig. 1A), grouped in two major units: the "*Rotularia* units" (Klb 2 to 6) and "Molluscan units" (Klb 7 to 10) (Macellari, 1988). The López de Bertodano Formation is currently assigned to a Maastrichtian to Danian age based on biostratigraphic correlations and magnetostratigraphy (Crame et al., 2004; Olivero, 2012; Tobin et al., 2012). It is important to remark the presence of the Cretaceous–Paleogene (K/Pg) boundary, located approximately between Klb 9 and Klb 10 (Zinsmeister, 1989, Fig. 1A, B). Their Upper Cretaceous fossil content includes abundant invertebrates represented by annelids such as *Rotularia*, bivalves, gastropods, ammonoids (Macellari, 1988; Zinsmeister, 1989) and decapods (Feldmann et al., 1993), among others. Vertebrates are also frequently found, and include the chondrichthyans *Notidanodon dentatus*, *Ischyodus dolloi*, *Chimaera zangerli*, *Callorhinchus torresi* and *Chlamydoselachus tatere* (Cione and Medina, 1987; Kriwet et al., 2006; Martin and Crame, 2006; Otero et al., 2013, 2014b), actinopterygians (Cione et al., 2018), mosasaurs such as *Plioplatecarpus* and *Mosasaurus* (Martin and Crame, 2006; Fernández and Gasparini, 2012), plesiosaurs such as *Morturneria seymourensis* (Chatterjee and Small, 1989; O'Keefe et al., 2017), several specimens assigned to indeterminate aristonectines and other elasmosaurids (Otero et al., 2014b; O'Gorman and Coria, 2017; O'Gorman et al., 2016, 2017), dinosaurs (Rich et al., 1999) and birds (Chatterjee, 2000; Hospitaleche and Gelfo, 2015).

The López Bertodano Formation was deposited on a marine shelf with increasing depth towards the top of the formation, peaking below the K/Pg boundary. Therefore, unit Klb 9 presents a character most associated with "off-shore" conditions compared to lower levels. The presence of an associated glauconite level located between Klb 9 and Klb 10 indicates a depth between 100 and 500 meters (Macellari, 1988).

The stratigraphic position of MLP 89-III-3-1 is approximately 2.3 m or less below the K/Pg boundary. The rate of sedimentary deposition in the upper part of the López de Bertodano Formation is about 0.15 mm/year (Tobin et al., 2012), and therefore 2.3 m represents ca. 15,000 years. However MLP 89-III-3-1 is located in a level with high concentration of glauconite, and therefore the sedimentary rate was probably lower in this level (Odin and Matter, 1981). However, even considering a sedimentary rate of 0.075 mm/

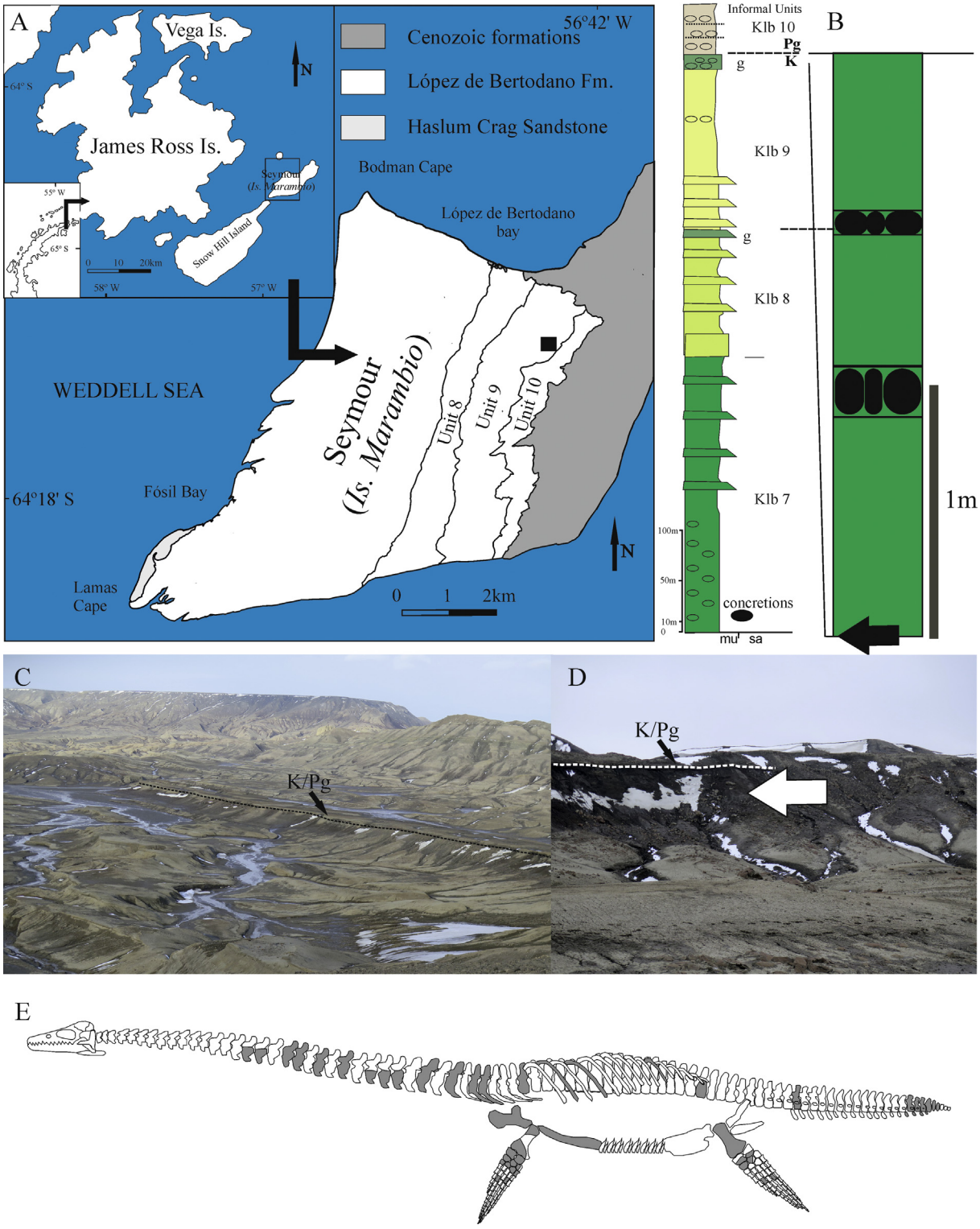

Fig. 1. **A**, Map showing the locality where MLP 89-III-3-1 was collected. **B**, Stratigraphic section indicating the provenance of MLP 89-III-3-1. **C**, **D**, Panoramic photo of locality, arrow indicate place of MLP 89-III-3-1. **E**, Diagram showing preserved elements of MLP 89-III-3-1 (map and stratigraphic section modified from Montes et al., 2013).

year, the specimen probably died approximately ca. 30,000 years prior to the K/Pg mass extinction.

3. Methods

The collection of MLP 89-III-3-1 was performed during several Antarctic campaigns since 1989 (2005, 2012 and 2017), a total of 800 kg of material was collected. The preparation of the specimen took three years because of the hardness of the matrix and was carried out mainly by the senior author (J.P.O'G). For the process jackhammers type ME 9100, 4 ½" angle grinder were used as well as hand tools and glue (cyanoacrylate and epoxy resin). The morphometric measurement indices used for the cervical vertebrae in the description are those proposed by Welles (1952), taking into account the length (L), the ratio of the height (H) and length ($100 \times H/L = HI$), the ratio of the breadth (B) and length, ($100 \times B/L = BI$) and the ratio of the breadth and height ($100 \times B/H$=BHI). Both breadth and height are measured in this study on the posterior articular faces. The Vertebral Length Index (VLI) [$L/(0.5 \times (H + B))$] (Brown, 1981) was also used; this indicates the degree of elongation of the vertebral body compared to height and breadth.

The growth stages interpreted follow the criteria of Brown (1981), who considered the fusion of neural arches to the centra as indicative of the "adult" stage, with a craniocaudal neurocentral fusion pattern during growth, and subsequently considering those individuals without fusion of these elements as a "juvenile" stage.

The length of the dorsal region (DL) is considered as a proxy of body size, precluding problems relative to the neck length. The length of the dorsal region (DL) is obtained as the sum of vertebral centrum lengths of the dorsal vertebrae. Where some dorsal vertebrae are not preserved, their length is inferred based on the average values of the preserved vertebrae (See Supplementary Data 1). In order to evaluate the correlation between dorsal region length (DL) and femur length (FL), a regression between DL and FL was performed. The significance of the correlation was evaluated using a Fisher statistical test (Press et al., 1992). All statistical test were performed using Past software (Hammer et al., 2001). Adding to this, the aristonectine skeleton SGO.PV.260 (*Aristonectes quiriquinensis*, referred) supports an increased number of dorsal centra, estimated as 24 for derived aristonectines (Otero et al., 2018).

4. Systematic paleontology

Sauropterygia Owen, 1860
Plesiosauria de Blainville, 1835
Plesiosauroidea Welles, 1943
Elasmosauridae Cope, 1869

Aristonectinae O'Keefe and Street, 2009 (*sensu* Otero et al., 2012)

cf. *Aristonectes* Cabrera, 1941

cf. ***Aristonectes*** sp.
Figs 2, 4–9, 13B

Type Species: *Aristonectes parvidens* Cabrera, 1941

Referred Specimen. MLP 89-III-3-1, postcranial skeleton (Fig. 1E) comprising nineteen well-preserved cervical vertebrae, one pectoral vertebra, fragments and natural casts of at least seven dorsal vertebrae and eight caudal vertebrae, left scapula, both coracoids; part of both humera, ulna and radius, carpal and metacarpal elements, femora, tibia and fibula, two tarsal elements, phalanges, ribs and gastroliths.
Locality and Horizon. Seymour (=Marambio) Island, Antarctica (64°16′15.5″ S; 56°43′01″ W). Upper levels of the López de Bertodano Fm, "Molluscan units", Klb 9 (Fig. 1B), upper Maastrichtian (Crame et al., 2004; Olivero, 2012).
Remarks. MLP 89-III-3-1 shows cervical centra with ventral notch in articular facets indicating elasmosaurid affinity (Fig. 2 A, B) and cervical centra as long as high and markedly wide, proportions recorded only in aristonectines (Cruickshank and Fordyce, 2002; Gasparini et al., 2003; Otero et al., 2014c). The cervical centra proportions of MLP 89-III-3-1 differ from those of *Kaiwhekea katiki* (Fig. 3, see Discussion) but are similar to those recorded for *A. parvidens* and *A. quiriquinensis*. Additionally MLP 89-III-3-1 shows radius longer than wide, differing from the wider than long radius of *Kaiwhekea katiki* (Benson and Druckenmiller, 2014:fig. 6c). MLP 89-III-3-1 also differs from *A. quiriquienensis* in 1] radius and ulna articular facets equal in length differs from the small and reduced radius facet for intermedium of *A. quiriquinensis*, and the shape of radial and distal carpals I, and 2] proximal projection of ulna that divides the epipodial foramen into one distal, larger sector and one much smaller proximal one, absent in *A. quiriquinensis*. However, the scarcity of material and the lack of overlapping material with the holotype of *A. parvidens* precludes MLP 89-III-3-1 being referred to *A. parvidens* or it being regarded as a new species. Unfortunately the other aristonectine from Antarctica, *Morturneria seymourensis* is based on a juvenile specimen that preserves only the skull and some anteriormost cervical vertebrae and therefore no comparison is possible (Chatterjee and Small, 1989). Taking into account these uncertainties for a direct comparison, and despite the similarities of MLP 89-III-3-1 with *Aristonectes* spp. a conservative nomenclatural position is followed and MLP 89-III-3-1 is referred to cf. *Aristonectes* sp.

5. Description

5.1. Ontogenetic stage

MLP 89-III-3-1 is considered an adult (*sensu* Brown, 1981) based on the presence of neural arches fused to the vertebral centra (Fig. 2B, E). The same criterion was used for assessing the adult condition of *Aristonectes parvidens* and *Aristonectes quiriquinensis* holotypes (MLP 40-XI-14-6 and SGO.PV.957, respectively). However, the holotype of *A. parvidens* shows the suture between the cervical ribs and cervical centra opened, or at least visible in some cervical vertebrae and the neural central closure is absent in caudal vertebrae. In MLP 89-III-3-1 studied here, even the hindmost caudal vertebra shows the neural arch fused to the centrum. Therefore, the closure sequence has reached a condition consistent with a comparatively more advanced growth stage.

5.2. General description

MLP 89-III-3-1 was collected dispersed over several meters throughout outcrops, as a consequence of recent weathering that gradually liberated the bone-bearing concretions from the poorly indurated pelitic sediment. The state of articulation is not homogeneous, comprising series of articulated vertebrae (Fig.4B, 5D) and carpal/tarsal parts, but also isolated elements. A few elements show some degree of weathering previous to the formation of the concretion, however, other elements show an unaltered bone surface.

5.3. Axial skeleton

The axial skeleton is partially preserved, lacking the sacral region and preserving only natural casts of a few dorsal vertebrae, but

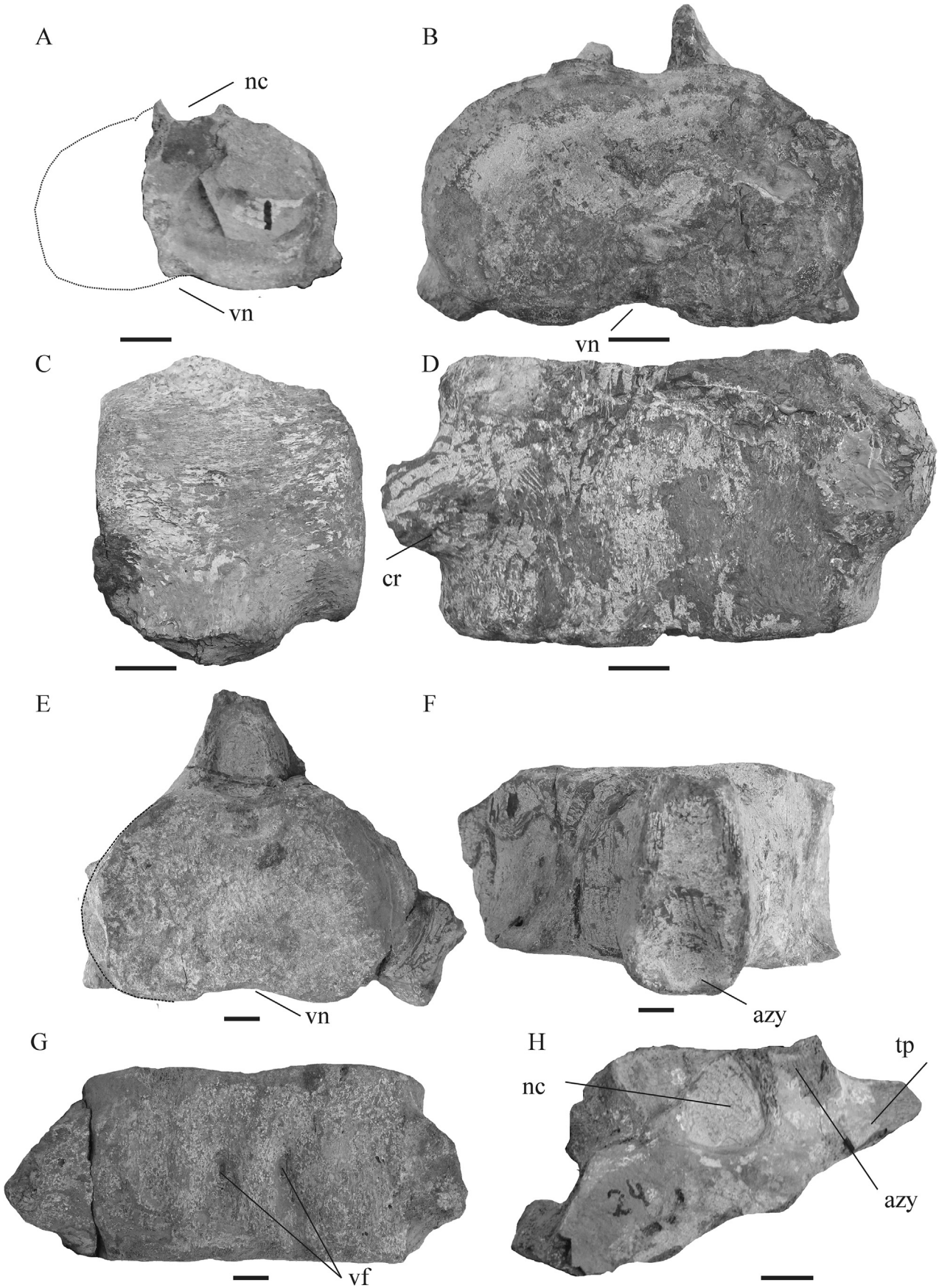

Fig. 2. MLP 89-III-3-1, cf. *Aristonectes* sp. **A**-**G**, cervical vertebrae. **A**, anterior cervical vertebra in anterior view. **B**-**D**, middle cervical vertebrae in **B**, posterior, **C**, right lateral view and **D**, ventral views. **E**-**G** posterior cervical vertebra in **E**, anterior, **F**, dorsal and **G**, ventral views. **K**, pectoral vertebrae in anterior view. Scale bars = 20 mm.

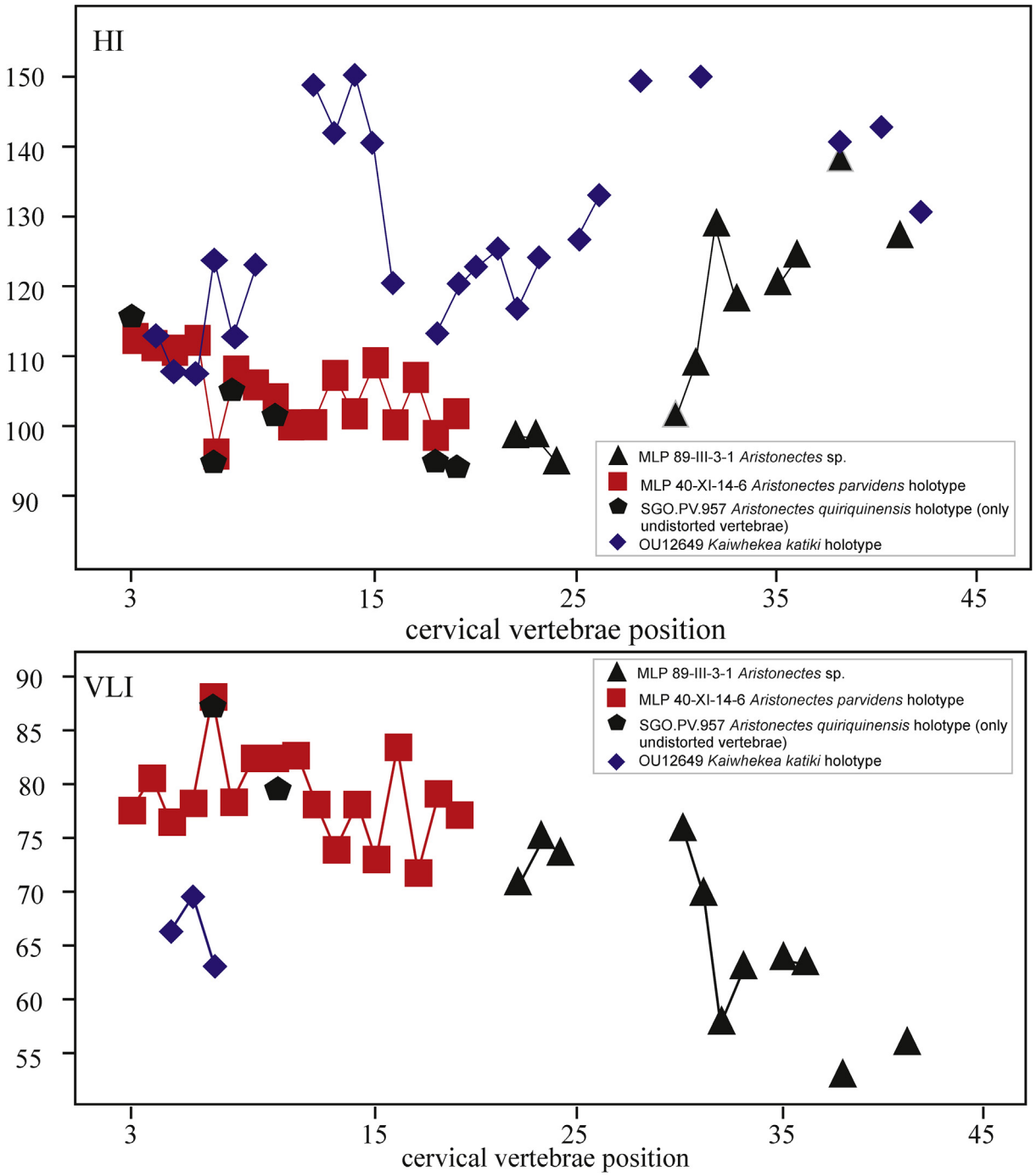

Fig. 3. Comparisons of cervical centra proportions of *Aristonectes parvidens* (MLP 40-XI-14-6); *Aristonectes parvidens* (SGO.PV. 967); cf. *Aristonectes* sp. (MLP 89-III-3-1) and *Kaiwhekea katiki* (OU 12549). Data taken from Otero et al. (2014c), O'Gorman et al. (2015) and Otero per obs. (2018).

partially preserving the cervical, pectoral and caudal regions (Fig. 1E).

5.3.1. Cervical region

The nineteen well-preserved cervical centra are higher than long and broader than high (Table 1). The articular faces are dumbbell shaped due the presence of a well-marked ventral notch (Fig. 2A, B, E). Cervical ribs of MLP 89-III-3-1 are fused with the centra, suggesting a comparatively more advanced state of maturity than that of the *A. parvidens* holotype (Fig. 2B). No clear lateral keel is observed, although in some cervical centra the lateral surface shows a change in slope similar to a lateral keel but without the dorsal and ventral concave areas. Ventrally there are two ventral foramina separated by a flat (anterior) to blunt (posterior) ridge (Fig. 2D, G). The anterior zygapophyses are medially fused in the midline (Fig. 2F) as is usual in elasmosaurids (Gasparini et al., 2003; Hiller et al., 2005; Sachs and Kear, 2015; O'Gorman et al., 2015). Only the neural spines of a few vertebrae are preserved as

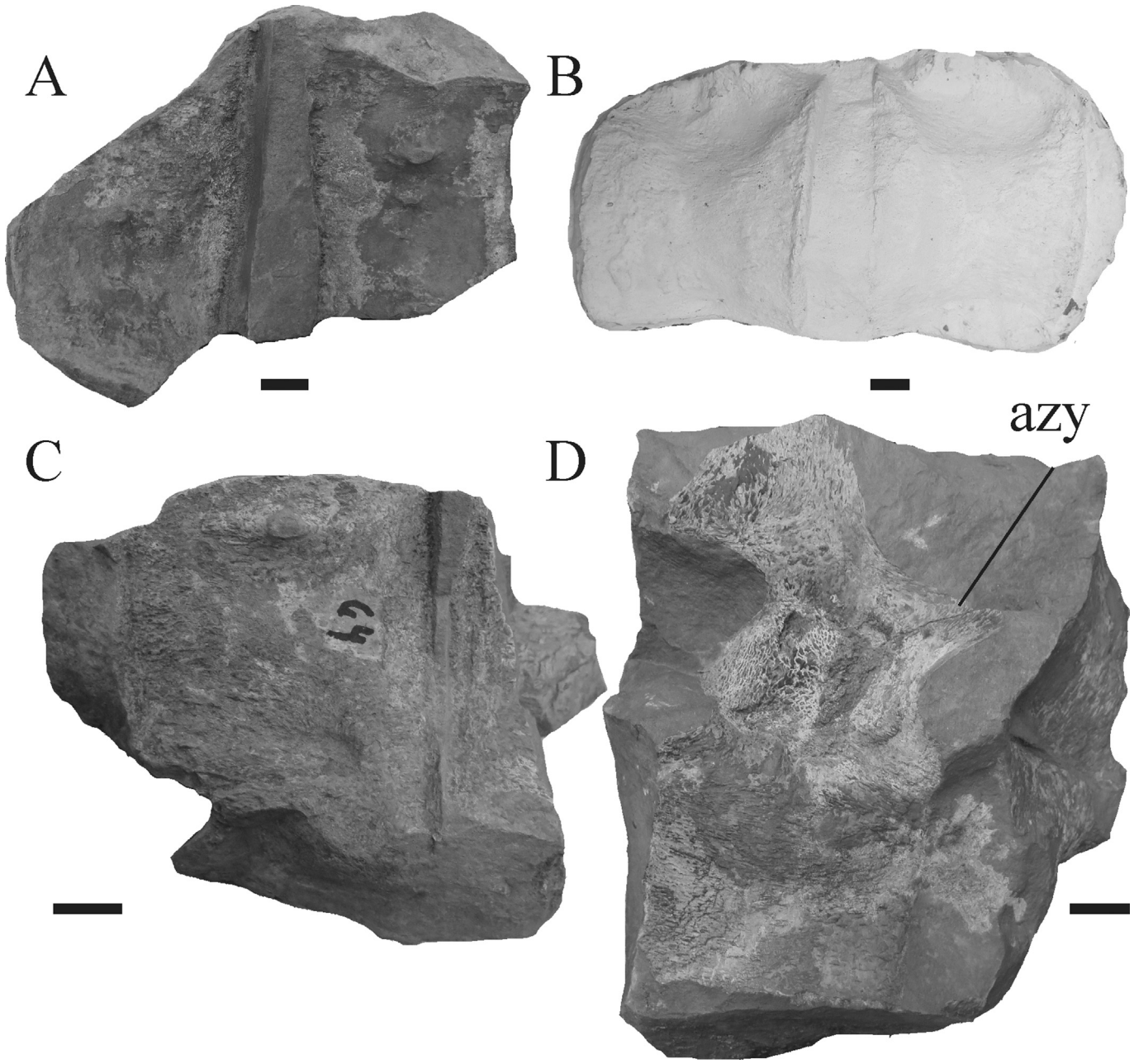

Fig. 4. MLP 89-III-3-1, cf. *Aristonectes* sp. dorsal vertebrae. **A**, **C** natural cast ventral surface. **B**, plaster cast of dorsal vertebrae in lateral view. **D**, natural cast and bone surface of dorsal vertebrae. Scale bar = 20 mm.

natural casts, showing that at least in the middle of the cervical region the neural spines are at least twice as high as the vertebral centrum.

5.3.2. Pectoral-dorsal region

The only preserved pectoral vertebra is incomplete. The neural canal is tear-shaped. The transverse process is stocky and slightly recurved caudally (Fig. 2H). There are at least seven preserved dorsal vertebrae represented by fragments and natural casts (Fig. 4). The lateral and ventral surfaces are concaveanteroposteriorly.

5.3.3. Caudal region

There are eight caudal vertebrae preserved. One group of three belongs to the middle zone of the caudal region. The morphology of the caudal vertebrae of MLP 89-III-3-1 is similar to that recorded for *A. parvidens* (MLP 40-XI-14-6), showing a high articular facet and large circular parapophysis (Fig. 5A, B). Other features are impossible to describe because of the poor preservation. Another partial caudal series seems to be the posteriormost caudal vertebrae because of the rapid decrease of the vertebral measurements (Fig. 5D). In all these caudal vertebrae the neural arches and the caudal ribs are fused to the centra. However, the hemal arches remain free and have not been preserved. Ventrally there is one foramen in each of the second and third vertebrae of this group. In the second, third and fourth vertebrae of this series there are strong muscle scars (fig. 5C) located in a convex zone on the side of the neural arch. The hindmost preserved vertebra shows ventrally projecting hemal facets (Fig. 5E, F). The caudal ribs are craniocaudally long, dorsoventrally extended in their proximal part and compressed distally (Fig. 5D).

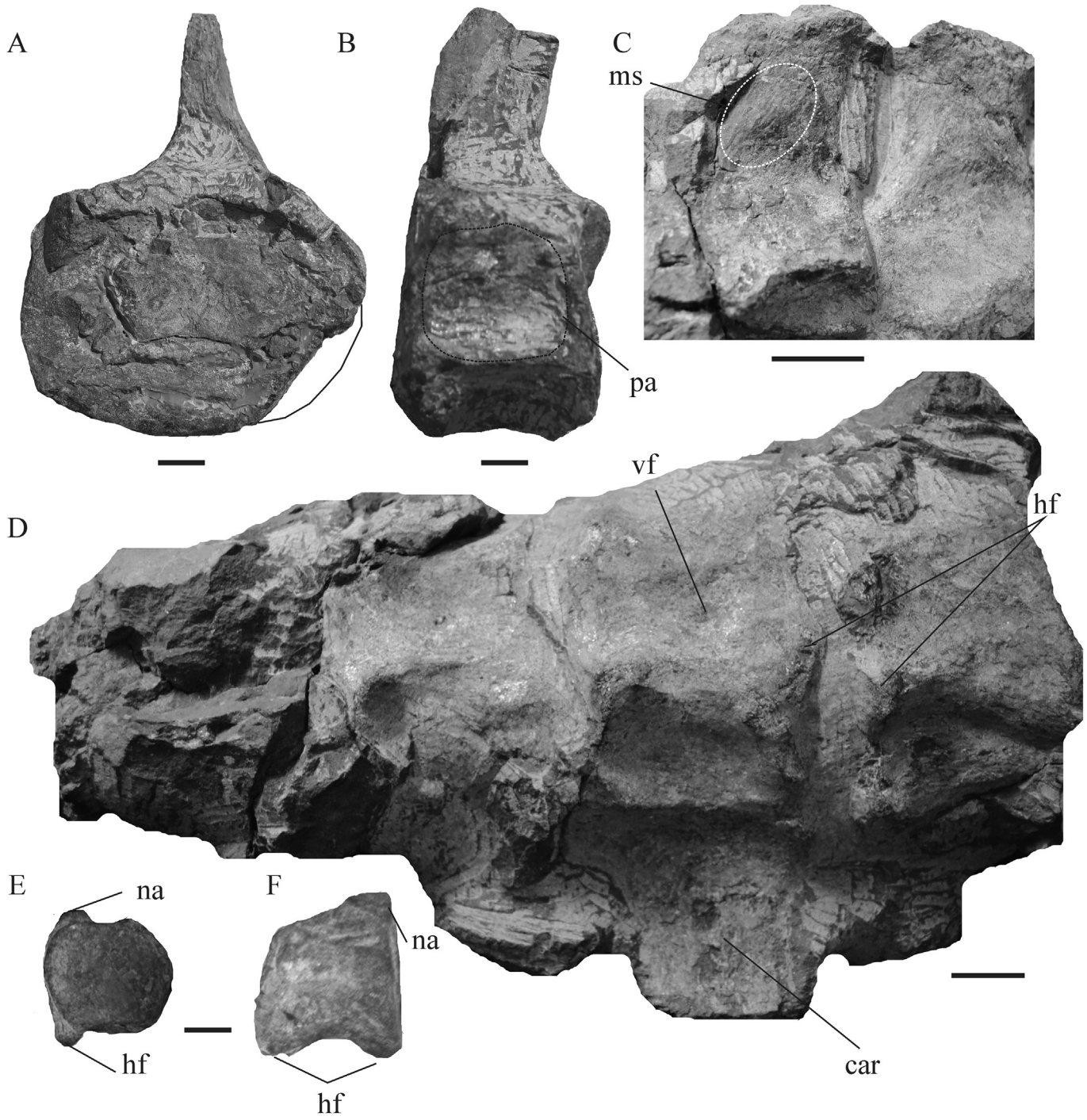

Fig. 5. MLP 89-III-3-1, cf. *Aristonectes* sp. **A-B**, middle caudal vertebra in **A**, posterior and **B**, left lateral views. **C**, detail of muscle scar on neural arch of middle caudal vertebra. **D**, posterior caudal vertebrae in ventral view. **E-F**, posteriormost preserved caudal vertebrae in **E**, anterior and **F**, right lateral view. Scale bar = 20 mm.

5.4. Appendicular skeleton

5.4.1. Pectoral girdle

The scapula shows the typical structure observed in elasmosaurids, a tri-rradiate element composed of a glenoid and ventral ramus and a dorsolateral process (Welles, 1943, Fig. 6). The glenoid facet is only slightly concave. The coracoid facet has little convex zones that indicate the presence of cartilage. The dorsolateral process is anterioposteriorly expanded and rectangular shaped in the distal part, without distal tapering (Fig. 6A). The dorsolateral and ventral form an angle of about 150° (Fig. 6D). As the anterior border is not completely preserved it is not possible to determine whether there was or not a scapular symphysis.

Only part of the medial ramus and posterior ramus of both coracoids are preserved. The available elements show the presence of a mid-ventral process and the coracoid posterior process forming the intercoracoid fenestra (Fig. 6E, F).

5.4.2. Forelimb

Humeri are represented by both humeral heads and one distal end. The humeral capitulum and tuberosity are partially confluent and form an angle of 90° in anterior view (Fig. 7A). The

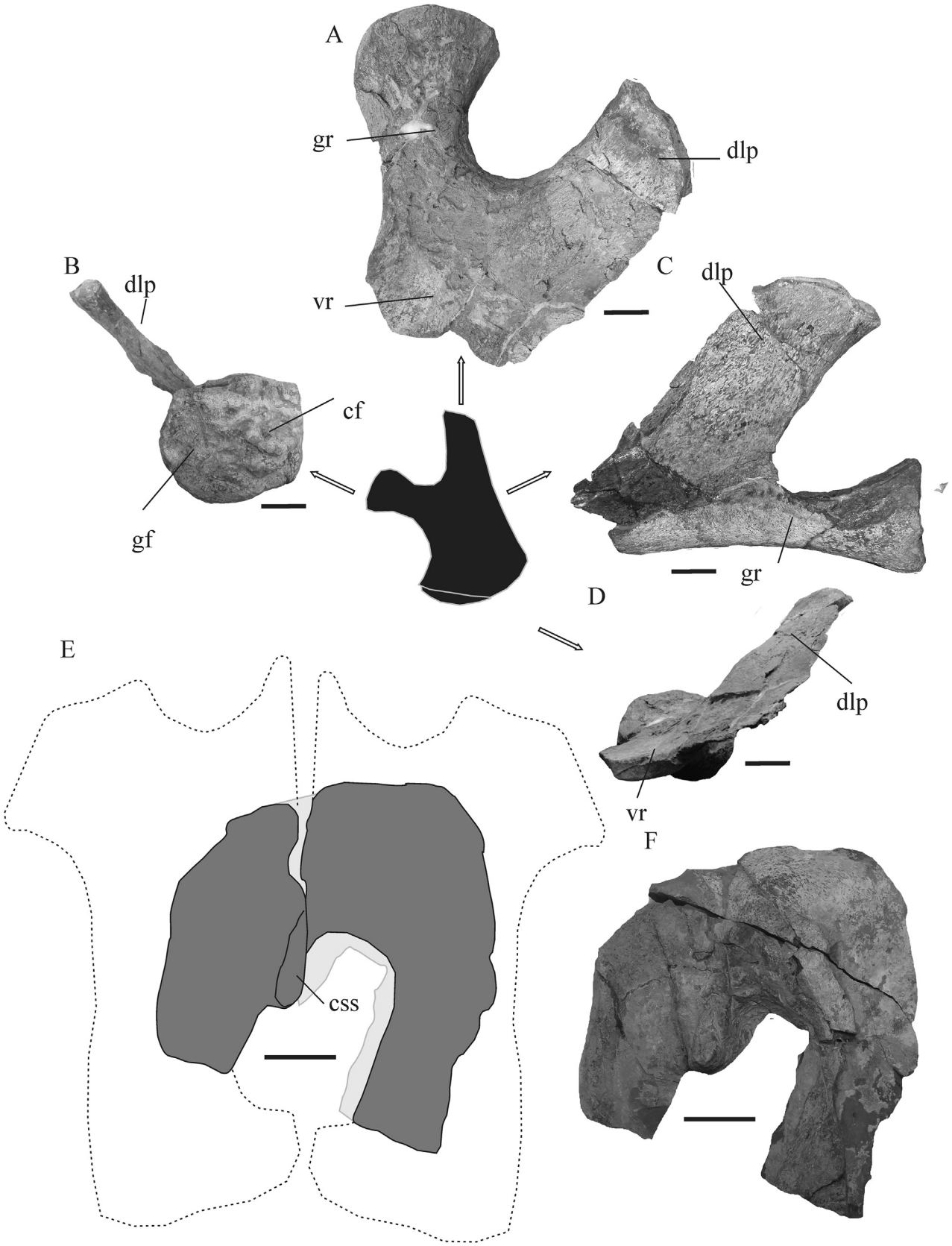

Fig. 6. MLP 89-III-3-1, cf. *Aristonectes* sp. **A-D**, scapula in **A**, dorsal, **B**, posterior, **C**, left lateral and **D**, anterior views. **E-F**, coracoids in dorsal? view. **E**, diagram and **F**, photo. **A-D**, Scale bar = 40 mm; **E**, **F,** Scale bar = 100 mm.

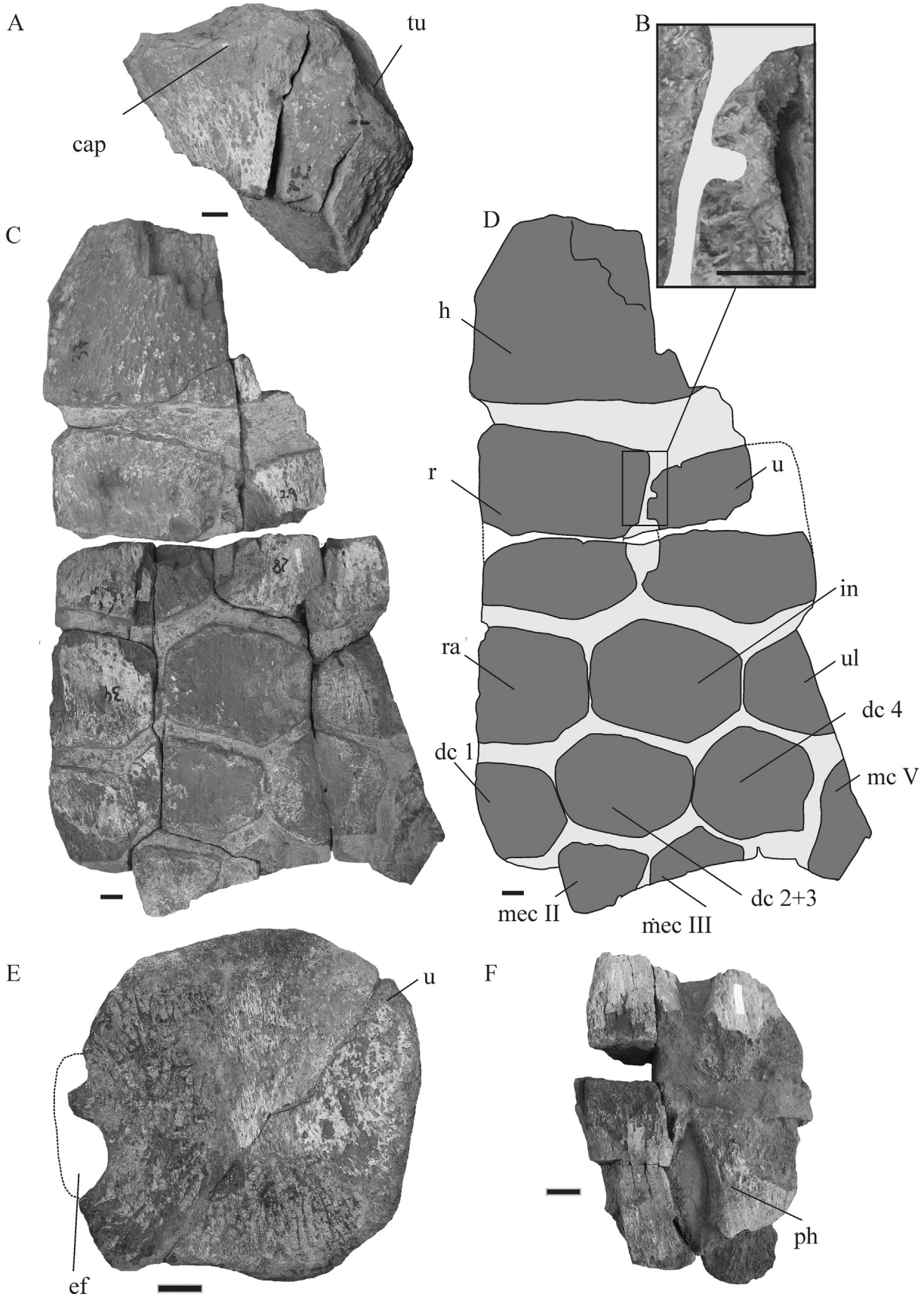

Fig. 7. MLP 89-III-3-1, cf. *Aristonectes* sp. **A**, humeral proximal end. **B**, detail of proximo-medial zone of ulna. **C-D**, humerus distal end, radius, ulna, carpal elements and metacarpals, **C**, photo and D, diagram. **E**, left ulna in dorsal view and **F**, phalanges. Scale bar = 20 mm.

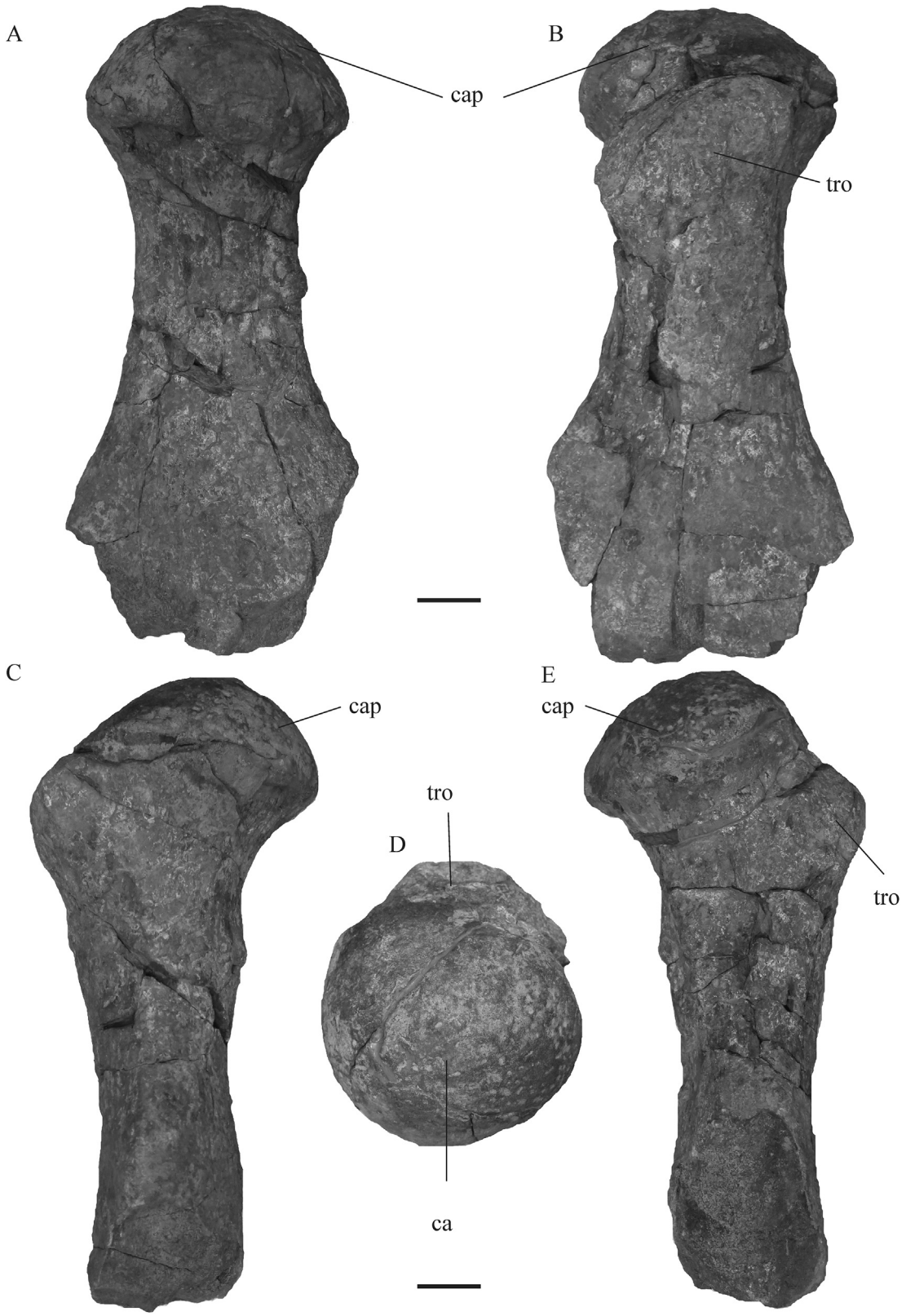

Fig. 8. MLP 89-III-3-1, cf. *Aristonectes* sp. **A-E**, right femur in **A**, ventral, **B**, dorsal, **C**, anterior, **D**, proximal and **E**, posterior views. Scale bar = 50 mm.

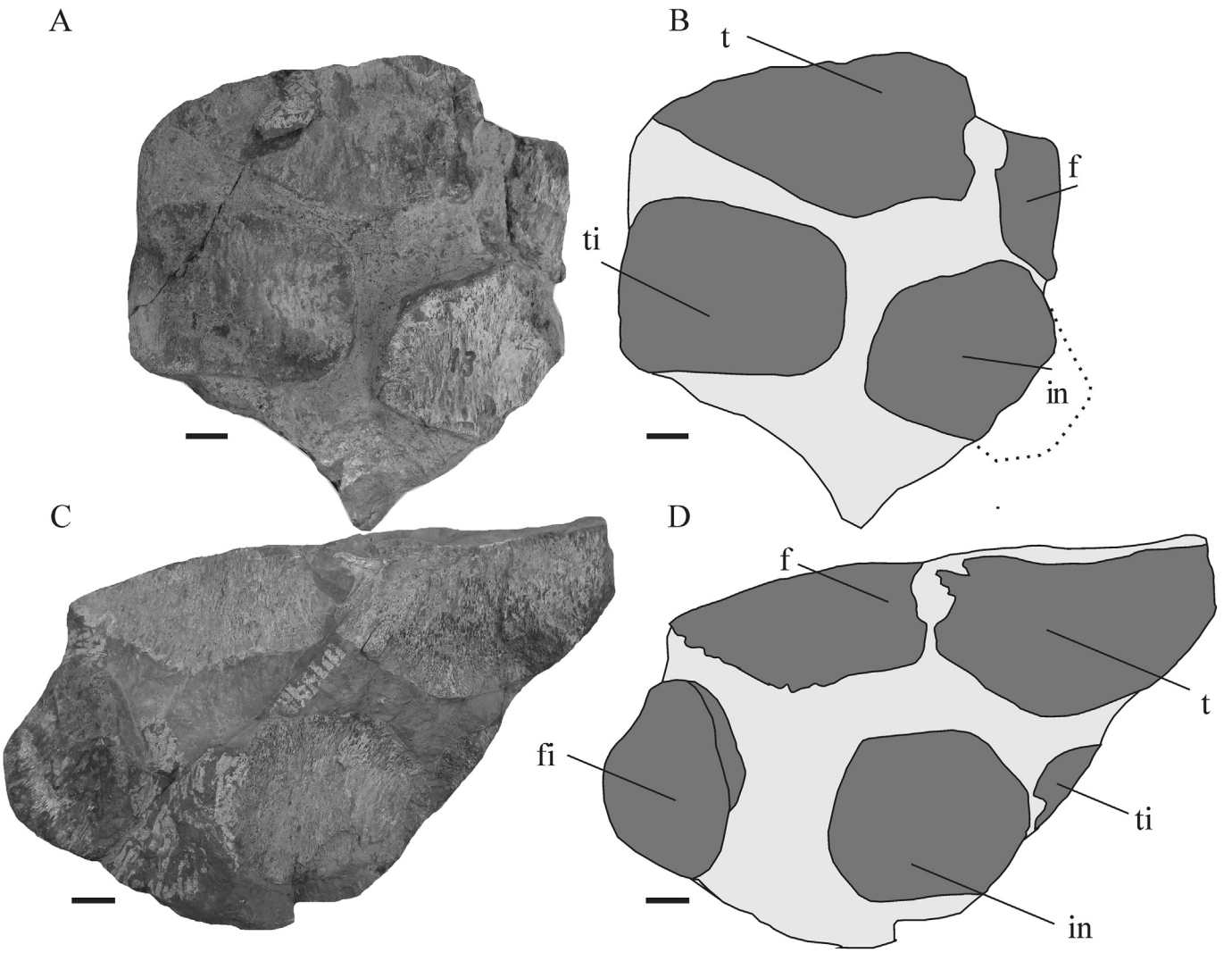

Fig. 9. MLP 89-III-3-1, cf. Aristonectes sp. **A**, **B**, left? tibia, fibula, tibiale and intermedium, **A**, photo and **B**, diagram **C**, **D**, right tibia, fibula, fibulare, intermedium and tibiale. Scale bars = 20 mm.

capitulum and tuberosity are only slightly convex (Fig. 7A). Therefore the capitulum is not hemispherical as is the capitulum of the femur (Fig. 8A); this differs from that recorded for *A. quiriquinensis*, but it is possible that MLP 89-III-3-1 is affected by taphonomic distortion. The distal end of humerus shows a small anterior expansion or "knee" (Fig. 7C, D). The angle between the radial and ulnar facets is difficult to assess but seems to be between 150° and 170°.

The radius is longer than wide (Fig. 7C, D), as occurs in *Aristonectes* spp. but differing from *K. katiki* (Benson and Druckenmiller, 2014:fig. 6c). The radius forms an elongated epipodial foramen (Fig. 7C, D) while the ulna is almost as long as wide. One interesting feature of the ulna is the presence of a small anterior, medially extended projection that divides the epipodial foramen in two parts, one somewhat smaller dorsal and a larger ventral part (Fig. 7B, C, E, F). This feature is observed in both ulnae of MLP 89-III-3-1 but it is not recorded in *Ar. quiriquinensis* or *Kaiwhekea katiki* (J.P.O'G and R.O. pers. obs.).

The intermedium is hexagonal shaped. The ratio between ulnar and radial facet lengths is ca. 1.3 (Fig. 7C, D). The distal carpal 1 shows a projection beyond the level of the metacarpal elements. The distal carpal 2 + 3 is wider than long.

5.4.3. Hind limb

Both femora are preserved. The left one is represented only by parts of the capitulum but the right femur is almost complete, therefore the description is based on it. The femur is 540 mm in length, relatively stocky element but with a well-defined shaft. The capitulum is strongly hemispherical (Fig. 8A, B, D). The tuberosity is not completely confluent with the capitulum (Fig. 8B). In dorsal view, the tuberosity is displaced to the posterior margin and is obliquely directed in relation to the proximo-distal axis of the femur (Fig. 8B).

The anterior margin of the femur shaft is more dorsoventrally concave than the posterior one (Fig 8C, E). The ventral shaft surface is markedly convex and shows a large muscle scar projecting from the general surface of the shaft (Fig. 8A). This muscle scar is displaced towards the posterior margin of the shaft; this insertion is probably associated with the puboischiofemoralis externus and the ischiofemoralis externus (Carpenter et al., 2010). The ventral surface of the shaft is comparatively more concave than its dorsal surface. The distal end is poorly preserved, making it impossible to know the exact shape of the distal articular facets.

Both hind limbs are represented by the distal part of epipodial elements and part of the mesopodium (Fig. 9). The tibia and fibula

Table 1
MLP 89-III-3-1. *Aristonectes* sp. Measurements and indexes of vertebral centra (in mm). In italics approximate values. C, cervical; D, dorsal; D, dorsal; Ca, caudal. ReP, relative position.

ReP.	L	H	B	HI	BI	BHI	VLI
C1	76	75	138	98.68	181.58	184.00	71.36
C2	81	80	135	98.77	166.67	168.75	75.35
C3	80	76	140	95.00	175.00	184.21	74.07
C4	93						
C5	95						
C6	90						
C7	95						
C8	100						
C9	100	102	161	102.00	161.00	157.84	76.05
C10	97	106	170	109.28	175.26	160.38	70.29
C11	89	115	190	129.21	213.48	165.22	58.36
C12	97	115	190	118.56	195.88	165.22	63.61
C13	95	115	180	121.05	189.47	156.52	64.41
C14	96	120	180	125.00	187.50	150.00	64.00
C15	90	125	210	138.89	233.33	168.00	53.73
C16			215				
C17	98	125	220	127.55	224.49	176.00	56.81
D1	95						
D2	100						
D3	105						
D4	110						
D5	120						
Ca1	83	110	150	132.53	180.72	136.36	63.84

enclose an epipodial foramen. The tibiale is a subrectangular element, wider than long (Fig. 9A, B). The intermedium shows tibial and fibular facets similar in size (Fig. 9A-D). There are several phalanges preserved but it is impossible to know to which limb they belong. All are constrained in the midline and show flat proximal and distal ends (Fig. 7F).

6. Calculation

Pearson's product-moment correlation coefficient = r (Press et al., 1992) was calculated between the DL and FL values (Table 2). The r obtained is 0.9047; this value is statistically significant at $\alpha = 0.05$. The regression between the DL (mm) and FL (mm) values result in the regression line (significant at $\alpha = 0.05$).

$$DL = 6.7358 \times FL - 716.69 \text{ mm (Eq 1; Fig. 10)}.$$

7. Discussion

7.1. Systematic affinities

The cervical vertebrae were ordered following the criterion of O'Gorman (2013). Fig. 2 shows that the sequence of VLI values decreases in the cranio-caudal direction. This pattern of decreasing indicates that the cervical sequence of MLP 89-III-3-1 belongs to the posterior part of the neck region where a decrease of the VLI value occurs in all elasmosaurids (data taken from Welles, 1952; O'Keefe and Hiller, 2006).

Determinations of plesiosaur specimens at the generic level without cranial material present great difficulty due to the strong similarity of postcranial elements. However, in this case the morphological peculiarities described indicate clear elasmosaurid affinities, and even more, aristonectine affinities. Among the latter, only two known genera could be directly compared with MLP 89-III-3-1; these are *Aristonectes* and *Kaiwhekea*, which are the only known adult aristonectine specimens that show relatively large body sizes. The latter two taxa share a unique combination of features such as the presence of anterior cervical vertebrae with dumbbell shaped articular faces, having a low VLI (averaging less than 80; Gasparini et al., 2003; Cruickshank and Fordyce, 2002; Otero et al., 2014c). A brief comparison between *Kaiwhekea katiki*, *Aristonectes parvidens* and *Aristonectes quiriquinensis* is based on specimens considered adults (Cruickshank and Fordyce, 2002; Gasparini et al., 2003), thus these specimens can be used to compare vertebral centrum proportions (Brown, 1981). The HI values of the cervical vertebrae of MLP 89-III-3-1 are more similar to those of *A. parvidens* than to those of *Kaiwhekea katiki*. Additionally, VLI values of the anteriormost cervical vertebrae of *Aristonectes* are higher than those recorded for *Kaiwhekea katiki* and the anteriormost preserved cervical vertebrae of MLP 89-III-3-1 have VLI values closely comparable with those recorded for the middle part of the neck of *Aristonectes* (Fig. 3A, B). Two additional features should be considered. The presence of lateral ridges, a feature present in *A. quiriquinesis* but absent in *A. parvidens* and MLP 89-III-3-1 and the presence of well developed radial facet of carpal intermedium and well developed tibial facet in the tarsal intermedium, both present in MLP 89-III-3-1 but absent in *A. quiriquinensis*, and the anterior projection of ulna and fibula into the epipodial foramen, absent in *A. quiriquinensis*. There are also other differences between *A. quiriquinensis* and MLP 89-III-3-1, such as the different shape of radial and distal carpal 1 (Fig. 11). The radius of MLP 89-III-3-is longer than wide, a feature also recorded in *A. quiriquinensis* (Otero et al., 2014c) and in the non-aristonectine *Callawayasaurus colombiensis* (Welles, 1962) but different from other elasmosaurids, including *K. katiki* (J.P.O'G, pers.obs. 2018), Benson and Druckenmiller (2014).

The other aristonectines are difficult to compare with the MLP 89-III-3-1 as no comparable material are available. However *Alexandronectes* seems to be a medium size aristonectine, based on the skull size (Otero et al., 2016) and therefore it differs from MLP 89-III-3-1. The case of *Morturneria seymourensis*, also from the López de Bertodano Formation, is more complicated as it is based on skull and few anteriormost cervical of a juvenile specimen (Chatterjee and Small, 1989). Thus, a direct comparison is not possible. However the recent re-study (O'Keefe et al., 2017) of *Morturneria*

Table 2
Values dorsal region length (DL), femoral length (FL) and number of dorsal vertebrae (NDv) considered. FL of Aristonectes quiriquinensis estimated based on humerus length of SGO.PV.957.

Taxa and material	DL (mm)	FL (mm)	N Dv	Citation
Aristonectes quiriquinensis SGO.PV.957	1966	459.5	24	Otero et al. (2014c)
Thalassomedon haningtoni DMNH 1588	2540	440	25	Welles (1943)
Hydrotherosaurus alexandrae UCPM 33912	1467	360	17	Welles (1943)
Morenosaurus stocki LACM 2802	1476	360	17	Welles (1943)
Vegasaurus molyi MLP 93-I-5-1	1065.5	280	17	O'Gorman (2013)
Futabasaurus suzukii NSM PV15025	1277.2	299	17	Sato et al. (2006)
Albetonectes vanderveldei TMP 2007.011.0001	1800	380	16	Kubo et al. (2012)
Kawanectes lafquenianum MLP 71-III-13-1, MCS PV 4	664	171	15	O'Gorman (2016a)
DL Average value (mm)	1624.1			
DL Standard Deviation (mm)	612.5			

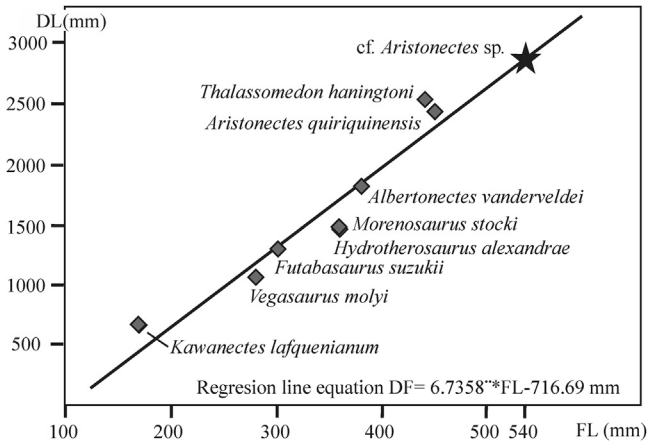

Fig. 10. Regression line of femur length (FL) on dorsal length (DL).

seymourensis shows that the specimen is indeed juvenile as previously pointed out by Chatterjee and Small (1989), but its ontogenetic stage is close to an adult condition, based in the presence of several well-defined morphological traits of the braincase (O'Keefe et al., 2017). Then, it can be segregated as a small-sized aristonectine compared to *Kaiwhekea katiki* and especially, compared to the larger *Aristonectes* spp.

The caudal vertebrae of MLP 89-III-3-1, although severely damaged, show a relatively high HI index like that recorded for *A. parvidens* (MLP 40-XI-14-6), with relatively large lateral parapohyses and octagonal articular faces (O'Gorman, 2016b). Unfortunately, no well-preserved caudal vertebrae are available in *Kaiwhekea katiki* and no adult specimen of *A. quiriquinensis* preserves them.

The scapula of MLP 89-III-3-1 shows a rectangular dorsolateral process, remarkably similar to that present in *A. quiriquinensis* (Otero et al., 2014c), and less similar to that of *Kaiwhekea katiki*, which has the dorsal end comparatively more rounded than that of *A. quiriquinensis*. Also it is slightly tapered dorsally, contrary to the expanded distal end of *A. quiriquinensis* and MLP 89-III-3-1 (Fig. 12). Additionally, the dorsolateral process of *K. katiki* is relatively longer than the one of *A. quiriquinensis* or the MLP 89-III-3-1. On the other hand, the scapula of *Ar. quiriquinensis* shows a robust dorsal process with a expanded distal end, having two well-marked facets. Its dorsal process is taphonomically bent; however, its total length is almost equal to the craniocaudal length of the scapula (Fig. 12).

Therefore the sum of evidence indicates more affinity of MLP 89-III-3-1 with *Aristonectes*. However, the scarcity of overlapping material precludes narrower comparisons, thus, no direct comparison could be made with *Alexandronectes* and *Morturneria* and for this reason open nomenclature is used and the MLP 89-III-3-1 is referred to cf *Aristonectes* sp.

7.2. Femoral hemispherical capitulum in a specimen referred to Aristonectes sp.

The holotype of *Aristonectes quiriquinensis* (SGO.PV.957) does not preserve the femoral capitulum and therefore it cannot be compared with MLP 89-III-3-1. The general shape of the femur in *A. quiriquinensis* has been inferred by an isolated femur (SGO.PV.135) that precisely matches the size, outline and three-dimensional features of the incomplete femur of the *A. quiriquinensis* holotype (Otero et al. 2015). This femur shows the presence of a hemispherical capitulum. This evidence was used by Otero et al (2015) to show that hemispherical capitula are present in different Weddellian elasmosaurids, including both aristonectines and non-aristonectines. Furthermore, this feature could be present in humeri and/or femora and it depends on the ontogenetic stage of the individuals, becoming progressively prominent in older individuals. The presence of a hemispherical capitulum adds to the taxonomic determination of MLP 89-III-3-1 as cf *Aristonectes* sp. This feature is present at least in *A. quiriquinensis*, (it cannot be verified in *A. parvidens*).

7.3. Body size of elasmosaurids

7.3.1. General background

Elasmosaurids appeared during the Early Cretaceous and radiated until the Late Cretaceous (Otero, 2016; O'Gorman, 2016a). During the last century and a half, the most discussed feature of this clade was their extremely long neck (O'Keefe and Hiller, 2006; Otero, 2016), whereas other features of the postcranium had been considered markedly conservative. However, the recognition of *Aristonectes* whitin the Elasmosauridae (Gasparini et al., 2003) indicates a previously unexpected morphological diversity, suggesting that elasmosaurids probably explored different ecological niches. One feature strongly correlated with ecology of species is its body size. However, body size variation among elasmosaurids has not been discussed in detail since Welles (1952). Body size is a concept associated with a scalar variable that could be measured using different proxies such as the trunk length, total body length and body mass. However, body length is not known for all elasmosaurid species and therefore the dorsal length (=trunk length, DL hereafter) is probably a better option for linear measurements. As DL does not consider the influence of the elongated neck, it is a better proxy for body mass.

7.3.2. Body length and body mass of MLP 89-III-3-1

One of the most striking features of MP 89-III-3-1 is its inferred large body size. The MLP 89-III-3-1 femur is larger than in any other elasmosaurid in both length and cross section (Fig. 13). A direct comparison shows MLP 89-III-3-1 likely among the largest elasmosaurids worldwide (Fig. 14). However, the incompleteness of the MLP 89-III-3-1 forces us to use estimation for the trunk length. In order to estimate the length of the dorsal region two methods were considered, one dependent on estimation of the number of dorsal centra, and other independent of it: 1] calculate the DL value as the product of the dorsal vertebrae number, considering 22 or 26 dorsal vertebrae based on the 24 dorsal centra recorded in *A. quiriquinensis* referred specimen SGO.PV.260, and the average length of the five preserved dorsal centra (105 mm) and 2] estimate the DL based on a regression line between femora length and DL in other elasmosaurids (See Fig. 10 and Calculation). The results of the application of these methods are: 1] = 22 × 105 mm = 2310 mm (22 dorsal vertebrae) and-26 × 105 mm = 2730 mm (26 dorsal vertebrae) and 2] = 2920 mm. To obtain a maximum and minimum estimations the promedium are calculated: (2310 m + 2920 mm)/2 = 2615 mm and (2730 mm + 2920 mm)/2 = 2825 mm.

Therefore the maximum and minimum estimation indicates this is among the largest elasmosaurids ever found in terms of trunk length (Table 2).

The holotype specimen of *Aristonectes quiriquinensis* (SGO.PV.957) was initially estimated at 8.5–9 meters long (Otero et al., 2014c). A recent revision (Otero et al., 2018) estimated a body length over 10 m. In order to estimate the total length of MLP 89-III-3-1, a new body length estimation of *A. quiriquinensisis* is given. Otero et al. (2014c) considered only 20 dorsal vertebrae but now it is known that the probable number is 24 (Otero et al., 2018), and these authors did not consider pectorals or sacrals as they were not originally prepared. The new estimation is indicated in Table 3.

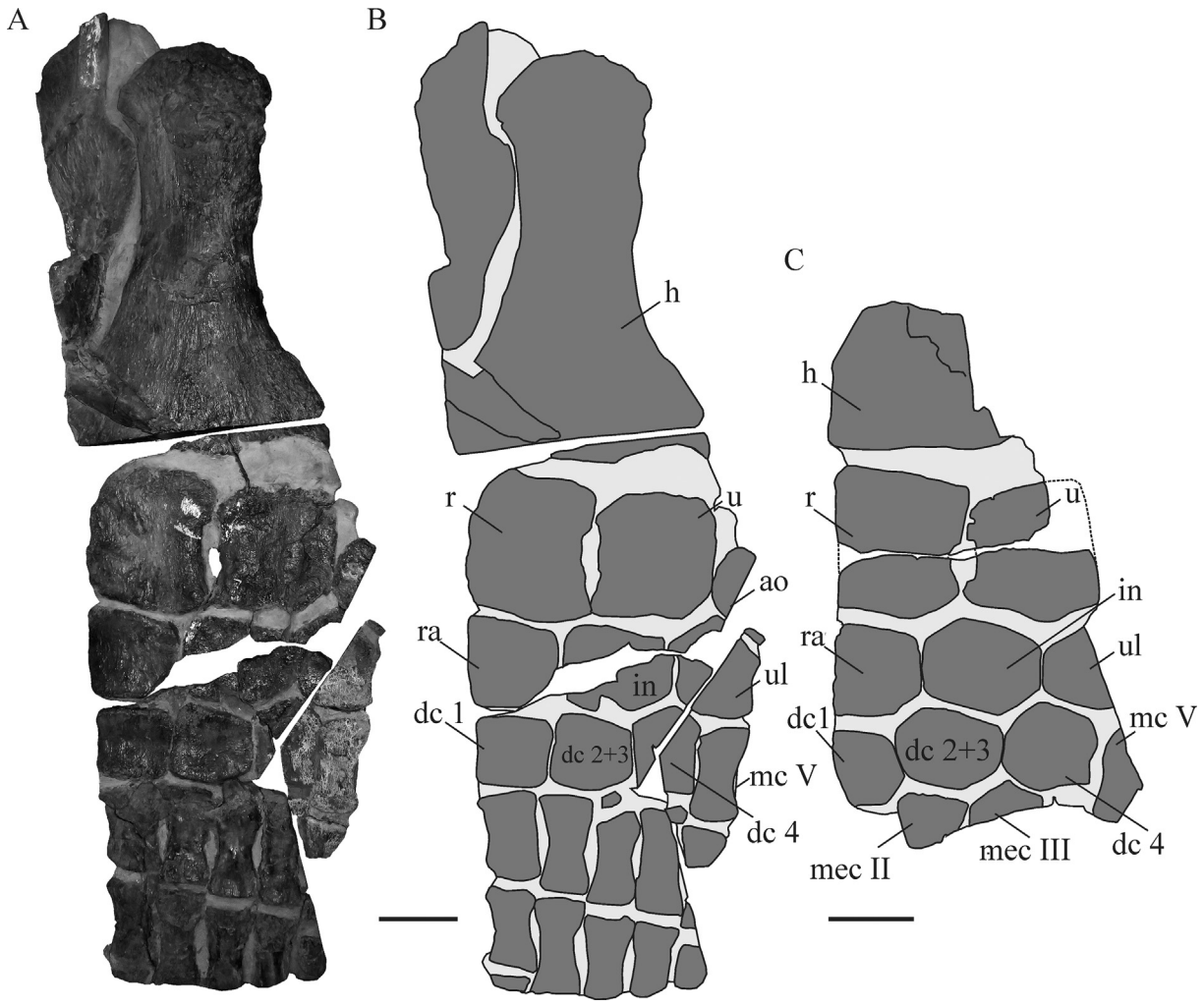

Fig. 11. Comparison between anterior limbs. **A**, **B**, *Aristonectes quiriquinensis* (SGO.PV.957), **A**, foto and **B**, diagram. **C**, MLP 89-III-3-1. cf. *Aristonectes* sp. diagram Scale bar = 100 mm.

Based on the different lengths of the respective dorsal region of each specimen, MLP 89-III-3-1 (2615 mm; 2825 mm) and SGO.PV.957 (2436.2 mm), and the body length estimated for *A. quiriquinensis* (10.232, Table 3) the body length of MLP 89-III-3-1 is estimated between 10.232 m × 2615 mm/2436.2 mm = 10.98 m and 10.232 m × 2825 mm/2436.2 mm = 11.86 m. Therefore MLP 89-III-3-1 is among the largest elasmosaurids, if we consider the body length of *Albertonectes vanderveldei* (11.6 m, adding a 400 mm skull to the estimation of Kubo et al., 2012); *Thalassomedon haningtoni* (10.86 m) and *Elasmosaurus platyurus* (10.29 m) (Welles, 1952).

The comparison of body proportions, considering the relatively short neck of the aristonectines and size and shape of several elements, indicate that MLP 89-III-3-1 shows a stocky morphology and therefore probably represents the elasmosaurids with the highest body mass. The estimation of body mass of plesiosaurs is a complex issue due to the necessity of complete specimens and the absence of available regression models. The previous estimation of the body mass of MLP 89-III-3-1 (O'Gorman et al., 2014) established a lower limit of 1300 kg with the objective of comparing with the mass of associated gastroliths recovered. However, the estimation follows the work of Everhart (2000) based on a long necked elasmosaurid and using an extremely low estimation of body length for MLP 89-III-3-1. Henderson (2006) estimated the length and body mass of *Cryptoclidus oxoniensis* to be 3 m and 217.9 kg respectively. Since the body shape and head/neck/trunk proportions of aristonectines are very similar to those of *Cryptoclidus oxoniensis* (see Henderson, 2006: fig. 1A and Otero et al., 2014c), we have used the same assumptions here and estimate the body mass of MLP 89-III-3-1 to be between 217.9 Kg × (10.98 m/3 m)^3 = 10,683.2 Kg and 217.9 Kg × (11.86 m/3 m)^3 = 13,463.2 Kg. Henderson considered the body length and body mass of *Thalassomedon haningtoni* (12 m, 5998 Kg), however if we used the estimation of Welles (1952; 10.85 m) the estimated body mass would be 5998 Kg × (10.86 m/12 m)^3 = 4445.82 Kg. Therefore, even though this is a rough estimation, it also provides evidence that MLP 98-III-3-1 is among the heaviest elasmosaurids ever recorded.

7.3.3. Body size diversity among elasmosaurids

In order to compare the DL of different elasmosaurids the DL were estandarized (SDL) following the formula: SDL = [(trunk length −(trunk length average value = 1624.1 mm)]/(trunk length standard deviation = 612.5 mm), see Table 2. Only *Thalassomedon haningtoni* and *Aristonectes quiriquinensis* and MLP 89-III-3-1 surpass the standardized value of 1 and only *Thalassomedon haningtoni* and MLP 89-III-3-1 have values over 1.5 (Fig. 15). On the other extreme, only *K. lafquenianum* plots below −1.5. These data show three interesting facts: first relatively large body sizes (SDL above 1)

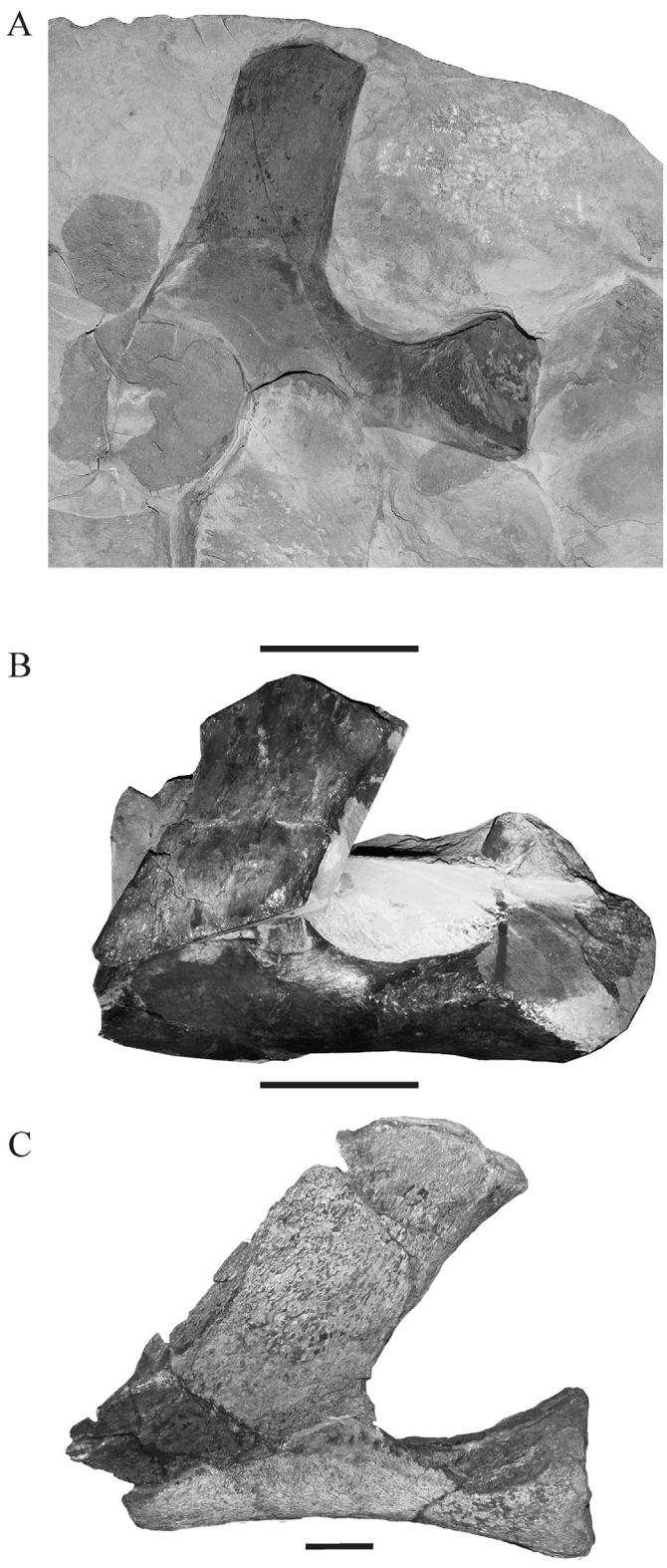

Fig. 12. Comparison of aristonectine scapulae. **A**, OU.12649, holotype of *Kaiwhekea katiki* Cruickshank and Fordyce (2002). Left scapula outline in dorsal view, mirrored for better comparison. **B**, SGO.PV.957, holotype of *Aristonectes quiriquinensis* Otero et al. (2014a), 204b, 204c. Right scapula in lateral view, mirrored for comparison. **C**, MLP 83-III-3-1, *Aristonectes* sp.; Left scapula in lateral view. **A**, **B**, Scale bar = 100 mm, **C**, Scale bar = 40 mm.

were achieved at least two times (*Thalassomedon haningtoni*, Cenomanian) and some aristonectines (Maastrichtian), both during the upper Cretaceous but separated by about 28 Ma and in groups with different body proportions (*Thalassomedon haningtoni*, non-elongated neck morphotype) and (Aristonectinae, aristonectine morphotype). However in both cases the trunk length increase is produced not only by an increase in vertebra size, but also by the acquisition of a larger number of dorsal vertebrae up to 25 (*Thalassomedon haningtoni*) and at least 24 (*Aristonectes quiriquinensis*). If we consider that the average value of dorsal vertebra counts in elasmosaurids other than *T. haningtoni* and the aristonectines is seventeen Table 2, the increases to 25 or 24 represent increases of nearly 50% in the number of dorsal vertebrae.

Second, extremely small body sizes were achieved at least twice, in *Nakonanectes bradti* and *K. lafquenianum* (see Serratos et al., 2017). Especially relevant is the conjunction of both extreme body size in the Late Cretaceous recovered in a single clade (Weddellonectia, O'Gorman and Coria, 2017), although see Serratos et al. (2017) and Sachs et al. (2018) for an alternative phylogenetic position of *Kawanectes lafquenianum*). However, independently of the internal phylogenetic affinities, the presence of the aristonectines and *Kawanectes lafquenianum* during the Maastrichtian interval indicates that body size diversity achieved its maximum (about 1.5 standard deviations from the mean) during the Maastrichtian, and therefore during the last six million years prior to the K/Pg mass extinction.

Finally, another observed pattern is the variable ratio between the femur length (FL) and dorsal length (DL), which shows a distinctive variation (Table 4), achieving higher values within the largest DL and FL (see *Thalassomedon haningtoni* and *Aristonectes quiriquinensis*). This tendency is clear considering Eq1: as follows:

$DL = 6.7358 \times FL - 716.69$ mm (Eq 1; Fig. 10).

$DL/FL = 6.7358 - 716.69$ mm/FL

Therefore, the ratio DL/FL increases as FL increases. This tendency requires further study in order to understand the relation between propulsion force given by limbs and trunk size.

7.4. Aristonectine morphology and trophic niche

Aristonectines show a highly derived group of features of both cranium and postcranium; and as previously discussed, some individuals could represent the heaviest elasmosaurids. This prompts the question: what is the biological role of these features? A simple observation reinforces the idea of a change in the prey capture strategy. This is suggested by the clear loss of the distance between the point of capture and the main body volume observed in other clades of Late Cretaceous plesiosaurs. Such features supposed and advantage in terms of prey capture, achieved in polycotylids by rostrum elongation and in elasmosaurids by the elongation of the neck region (O'Keefe and Hiller, 2006; O'Keefe, 2004). However, Aristonectines show increased head volume, reduction of the rostrum and symphysis length and a relative shortening of the neck that reduced its lateral mobility (Otero et al., 2014c, 2018; O'Gorman, 2016b; O'Keefe et al., 2017). The loss of these features, all related to approaching prey, strongly indicates a change in the entire strategy of prey capture.

The clarification of the role of the striking aristonectine prey-capture adaptations requires an integrative interpretation of all the aristonectine features. Several authors have mentioned the possibility of the use of the increased number of teeth and large skull as a system for sieve feeding (Chaterjee and Small, 1989; O'Keefe et al., 2017). Although, aristonectines probably did not feed on microplankton, as the sieve system formed by teeth seems to be poorly efficient for dealing with such prey sizes. Thus the option of mesoscopic invertebrates as a food source has been

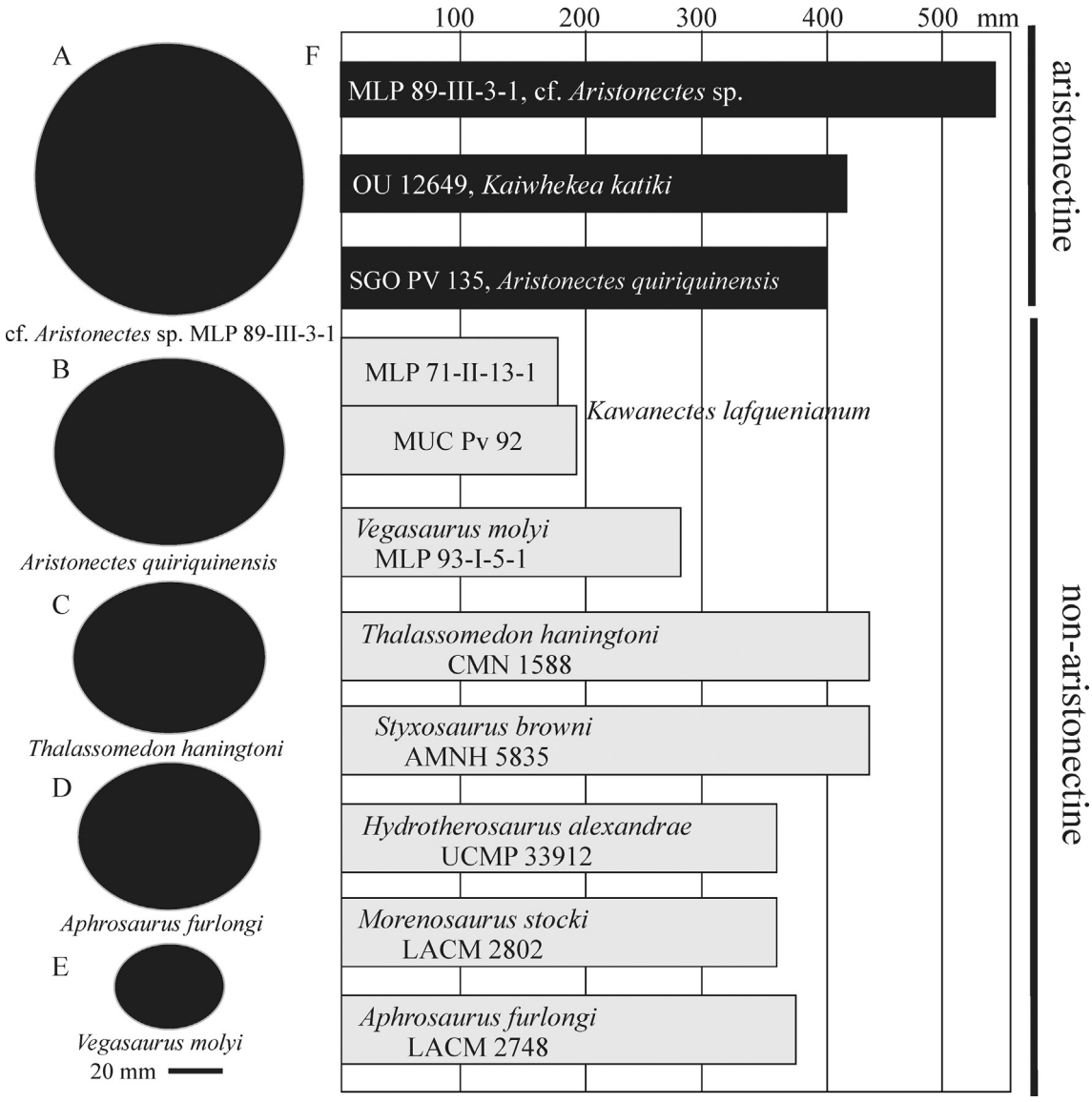

Fig. 13. Comparison of elasmosaurid femur sizes. **A-E**, minimum cross sections, **A**, MLP 89-III-3-1; **B**, SGO.PV. 135; **C**, DMNH 1588; **D**, LACM 2748; **E**, MLP 93-III-3-1. **F**, femur lengths (Data taken from Welles, 1943; Otero et al., 2014b; O'Gorman et al., 2015; Otero, 2016).

previously hypothesized (O'Keefe et al., 2017). Sanderson and Wassersug (1993) listed morphological features correlated with sieve feeders, but how well do these fit with aristonectine morphology? Here each one is discussed in terms of the aristonectinae features.

1] Relatively large head (from a quarter to a third of the total body length) and large buccal volume.

The cranial length in aristonectines is markedly smaller than a quarter of the total body length. However, as was commented previously, the total length of plesiosauroids is not a good indicator of body size because of the presence of a long neck. But considering only the dorsal region, the proportion is more similar to those recorded for sieve feeders. The ratio of skull length to dorsal region length can be calculated for the aristonectine SGO.PV.957, holotype of *Aristonectes quiriquinensis*, to be 100 × 0.989 m/2.4362 m = 40.6%. The same ratio calculated for the large typical long-necked elasmosaurid *Thalassomedon haningtoni* is 100 × 0.510 m/2.540 m = 20% (Skull length taken from Carpenter, 1999). Therefore aristonectines show increased skull size relative to the dorsal region. Additionally, several features of the aristonectine skull generate a large buccal volume such as the hooping of the mandible rami (O'Gorman, 2016b; O'Keefe et al., 2017), wider skull (O'Gorman, 2016b) and deep lateral arching of the palate (O'Keefe et al., 2017).

2] Reduced dentition.

Reduction of the dentition in terms of weak attachments and small tooth size has been also reported for aristonectines (O'Gorman, 2016b).

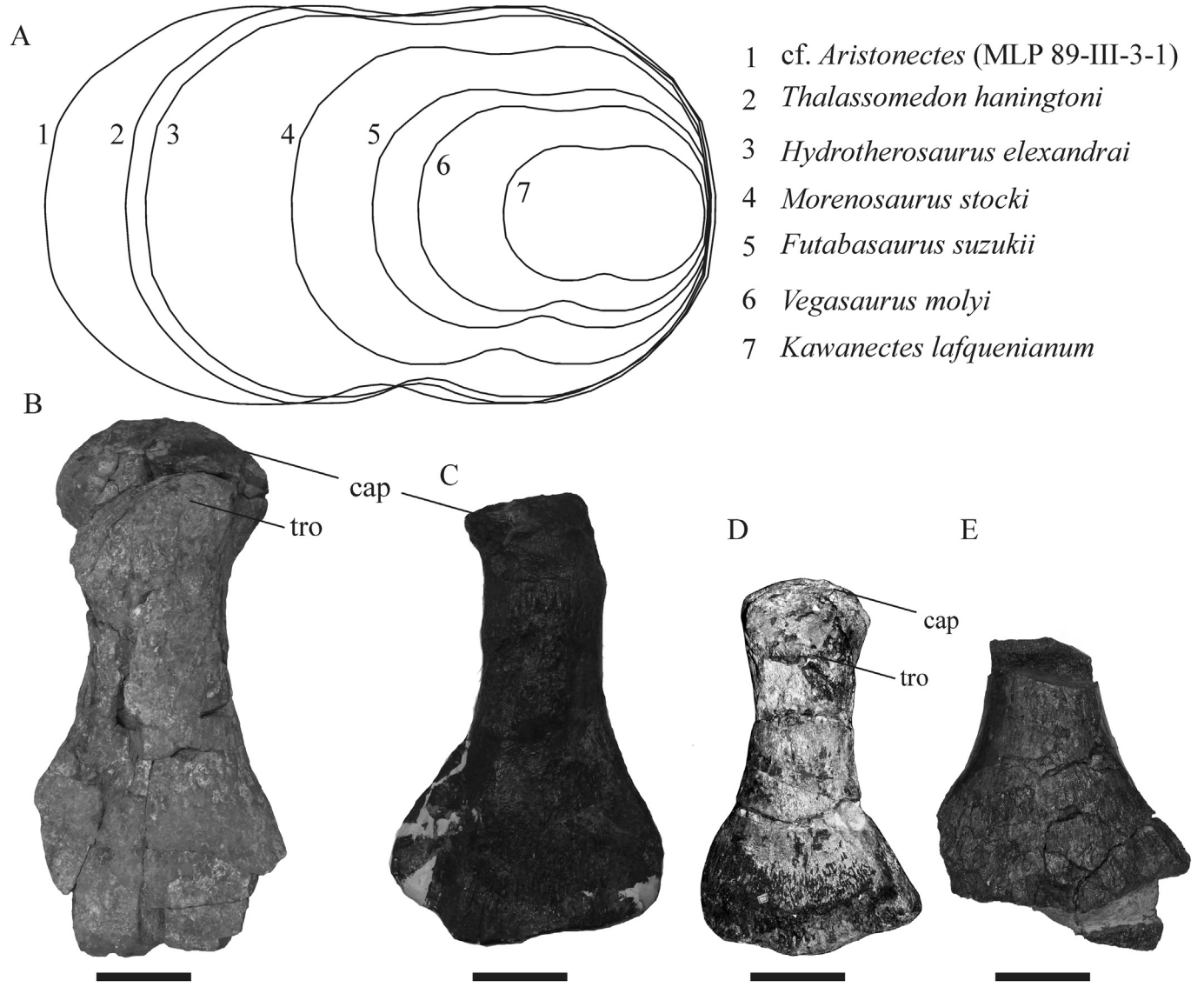

Fig. 14. Comparison of size of elasmosaurid postcranial elements. **A**. Scheme of articular face of hindmost cervical centra. **B-D,** femora in dorsal view, **B**, MLP 89-III-3-1 (cf. *Aristonectes* sp.), **C**, DMNH 1588, *Thalassomedon haningtoni*. **D**, SGO.PV. 135, **E** femur SGO.PV. 957 in ventral view. Scale bar = 100 mm. (Data taken from Welles, 1943; O'Gorman et al., 2015; O'Gorman, 2016a).

3] Small eyes and reduced orbit.

No reduction is observed in *Morturneria seymourensis* or *Kaiwhekea katiki* (Cruickshank and Fordyce, 2002; O'Keefe et al., 2017) and that could indicate that maybe vision was necessary to detect the preferred prey.

4] Large areas for epaxial muscle insertion and a short cervical region that resists downward torque on the head produced when the mouth is opened.

The aristonectines show a wide posterior part of the cranium able to receive the insertion of strong musculature. Additionally the

Table 3
Estimation of length of regions of axial skeleton of SGO.PV.957, *Aristonectes quiriquinensis* holotype.

Axial region	Measure	Data source
Skull	0.989 m	Estimated based on the skull of A. parvidens and the differences in length of cervical vertebrae of A. parvidens and A. quiriquinensis
Cervical	3.000–3.500 m (considering 3.25 m)	Otero et al. (2014c)
Pectoral	0.303 m	Estimated base on 3 × dorsal average length value (see Sup. Mat.).
Dorsal	2.4362 m	Estimated based on 24 × average length value (see Sup. Mat.).
Sacral	0.303 m	Estimated base on 3 × dorsal average length value (see Sup. Mat.).
Caudal	3 m	Otero et al. (2018)
Total	10.232 m	

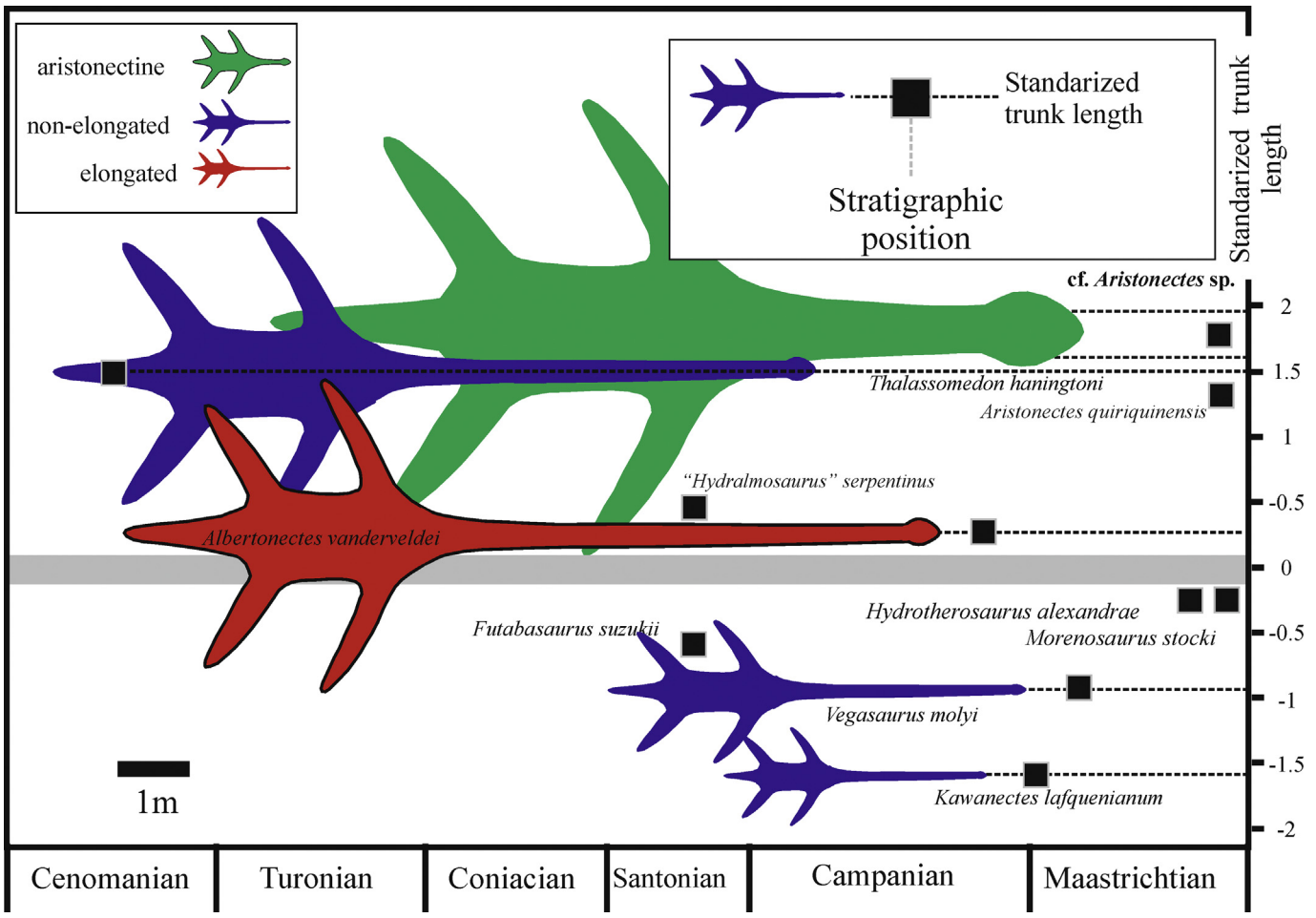

Fig. 15. Plotted of body size and ages of several Late Cretaceous elasmosurids.

position of the four anteriormost cervicals located far ahead due the strong medial embayment produced by squamosals also strengthens the anterior part of the neck and the connection with the head (Otero et al., 2014c; Otero et al., 2018). Furthermore, the aristonectines underwent a process of strengthening of the neck by the widening of the cervical centra, necessary to resist the drag forces during the engulfing of volumes of water or substrate (O'Gorman, 2016b).

5] Elongated and broadened jaw bones, not strongly ossified.

The mandible of the aristonectine is relatively gracile in relation to the skull size and the symphysis of *Kaiwhekea* and *Aristonectes* is relatively gracile compared to other elasmosaurids.

Table 4
Ratio dorsal length (DL)/femur length (FL) in several elasmosaurid taxa. Data taken from Welles (1943); Kubo et al. (2012); Otero et al. (2014c); O'Gorman et al. (2015); O'Gorman (2016a).

Taxa and specimen	DL/FL (mm)
Thalassomedon haningtoni DMNH 1588	5.78
Aristonectes quiriquinensis SGO PV 0.957	5.41
Albetonectes vanderveldei TMP 2007.011.0001	4.74
Futabasaurus suzukii NSM PV15025	4.26
Morenosaurus stocki LACM 2802	4.10
Hydrotherosaurus alexandrae UCPM 33912	4.07
Kawanectes lafquenianum MLP 71-III-13-1, MCS PV 4	3.88
Vegasaurus molyi MLP 93-I-5-1	3.81

This summary indicates that aristonectines show some features related to sieve feeders following the hypothesis of O'Keefe et al. (2017). Even more recently, Noè et al. (2017) indicated the possibility of sieve feeding or similar by other plesiosauromorphs. Two main features indicate they are not specialized on planktonic organisms: the separation between teeth is relatively small, not small enough to retain the smaller plankton but to capture small nektonic invertebrates such as juvenile cephalopods or crustaceans. The second feature is the lack of ocular reduction that indicates the necessity of vision, probably to detect this type of mesoscopic prey. In this context the development of large body sizes is correlated with a mechanical necessity of sustaining this large skull and the existence of a highly productive environment with concentration of small prey that probably drove the evolution of aristonectine morphology.

7.5. Body size, paleoenvironment and extrinsic drivers of aristonectine evolution

The size of MLP 89-III-3-1 and other aristonectines raises the question about the development of relatively large body sizes in this group compared to other Santonian-Maastrichtian elasmosaurids. This difference is more accentuated if body mass is considered. The attainment of large body size seems to be temporally correlated with a cooling trend of sea water in the Weddellian Province, one of the most marked environmental changes that occurred during the last part of the Late Cretaceous (Ditchfield

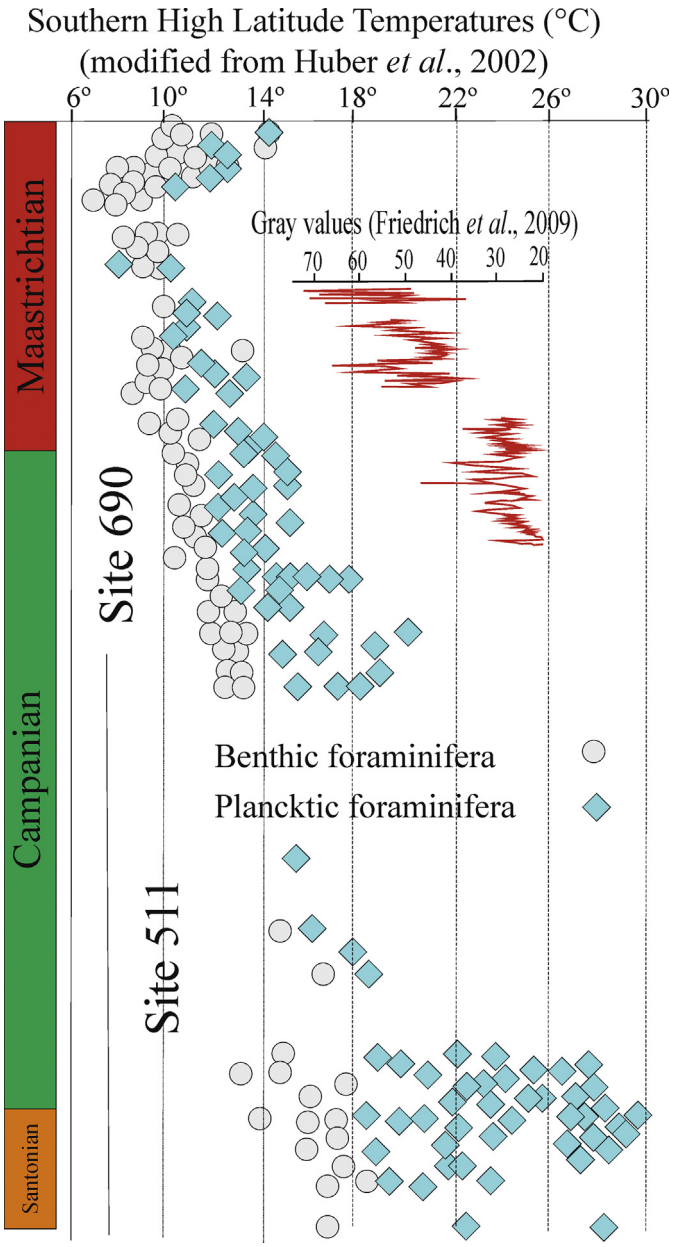

Fig. 16. Diagram showing sea temperature of the southern ocean and gray values of drill 690, indicating marine productivity (data from Hubert et al., 2002 and Friedrich et al., 2009).

et al., 1994; Dingle et al., 1998; Huber et al., 2002). This cooling process started from the Late Cretaceous maximum during the Coniacian–early Santonian (18 °C) and changed to values of ~10 °C and 8 °C or less in the late Maastrichtian, based on benthic foraminifera (Huber et al., 2002, Fig. 16). The decrease of polar sea water temperature generated a major ecological modification that could explain biological changes including the early extinction of several cosmopolitan taxa and the radiation of the kossmaticeratid ammonoids in Antarctica (Olivero, 2012), a probably stenothermal group of ammonoids that shows a radiation probably associated with the capacity to deal with the new thermal conditions. Also, the calcareous plankton paleodistribution in the southern oceans was probably influenced by this long-term cooling (Huber and Watkins, 1992). Therefore, it is not improbable that this change could have had a strong influence in the evolution of a new morphology among marine reptiles, even in a relatively conservative group such as the elasmosaurids.

The clarification of the possible connection between the rise of the aristonectines and the cooling trend of sea water during the Late Cretaceous requires an understanding of its effects in other elasmosaurid groups. The persistence of the more typical, non-aristonectine elasmosaurids in the Weddellian Province is very clear (Gasparini and Salgado, 2000; Hiller et al., 2005; O'Gorman, 2012; Otero et al., 2014a; O'Gorman et al., 2017). Thus there was no replacement of the non-aristonectines by the aristonectine elasmosaurids. Therefore, the body mass increase is not consistent with an explanation based on an ecomorphological "Bergman-like" rule. Instead, it is more probable that the aristonectines occupied a new niche that appears related to associated biotic changes generated by the cooling of the sea water (O'Gorman, 2016b; O'Keefe et al., 2017). The connection between these two elements (cooling trend of sea water and development of the aristonectine morphology) could be a peak of marine productivity associated with increases in water mixing, probably related to upwelling processes. Despite the difficulties in measuring ancient marine productivity, there is some evidence supporting increases in marine productivity in the Weddellian Sea during the Maastrichtian. Friedrich et al. (2009) recorded an increase of gray values (color spectrometer measure of drilling core) correlated with a positive $d^{13}C$ excursion detected in the Maastrichtian record of drill 690 (eastern Weddell Sea, southern South Atlantic Ocean; S 65°lat), possibly indicating an increased flux of calcium carbonate due to increased surface water mixing and marine productivity (Friedrich et al., 2009, Fig. 16). Additionally, the presence of MLP 89-III-3-1 with its relatively large body size and its trophic necessities suggests an environment with high primary productivity occurring stratigraphically close to the K/Pg boundary.

The body size increase in aristonectines, the development of their distinctive morphology and the modification of sea water

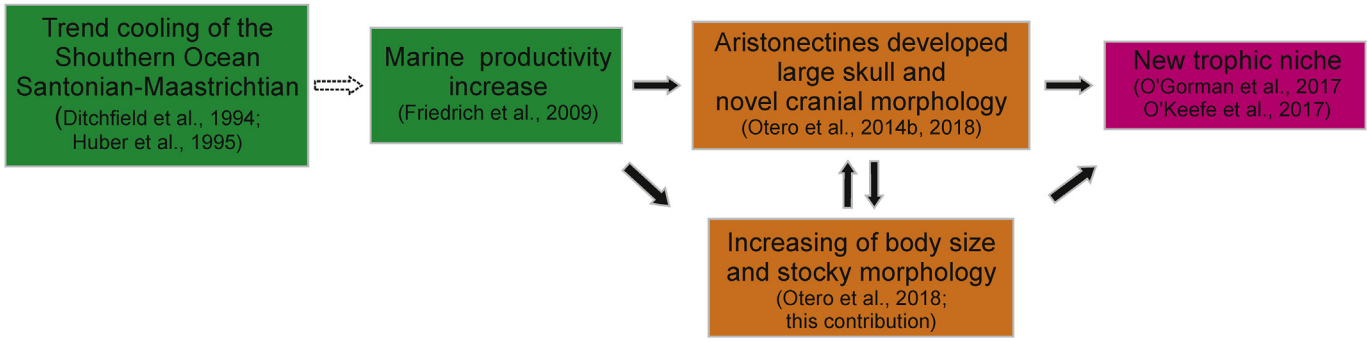

Fig. 17. Proposed evolutionary scenario of aristonectines.

conditions that could affect primary productivity, are temporally and spatially connected indicating some causal connection that could be used as a preliminary model of an evolutive scenario of the aristonectine clade (Fig. 17).

8. Conclusion

Aristonectines include the longest and heaviest elasmosaurids that ever existed. MLP 89-III-3-1 shows that they survived at high latitudes almost until the K/Pg boundary. Elasmosaurids achieved maximum body size diversity during the Campanian–Maastrichtian. The distinctive features of the aristonectines agree with those recorded for sieve feeders. The development of the aristonectine morphology, the increased body size and the cooling trend in the sea water are temporally and spatially correlated. The connection between these elements could be the change in marine conditions and especially the supposed increases in marine productivity that opened a new niche that was occupied by aristonectine elasmosaurids

Acknowledgements

This contribution was mainly funded by the Dirección Nacional del Antártico and the Instituto Antártico Argentino, project: PICTO 2010-0093. Partial funding was provided by the Consejo Nacional de Investigaciones Científicas y Tecnológicas, Agencia Nacional de Promoción Científica y Tecnológica, and Universidad Nacional de La Plata through PICT -20120748 and PICT 2015-0678. We thank the logistic support of the Fuerza Aérea Argentina. Thanks to E. Perez-Pincheira; N. Muñoz, L. Acosta-Burlaille and F. Solari-Orellana for partial fossil preparation. The authors thank Z. Gasparini for reading an earlier version of the manuscript, and B. Zinsmeister, J. Moly, P. Bona and M. De Los Reyes and J. Lusky for the Antarctic fieldwork and comments that improved this manuscript. RAO was supported by Proyecto Anillo Conicyt-Chile, ACT 172099. The authors thank the comments of the editor, two anonymous reviewers and S. Sachs (Naturkunde-Museum Bielefeld, Germany) that improved this contribution.

References

Benson, R.B., Druckenmiller, P.S., 2014. Faunal turnover of marine tetrapods during the Jurassic–Cretaceous transition. Biological Reviews 89, 1–23.
Brown, D.S., 1981. The English Upper Jurassic Plesiosauroidea (Reptilia) and a review of the phylogeny and classification of the Plesiosauria. Bulletin of British Museum of Natural History (Geology) 35, 253–347.
Cabrera, A., 1941. Un Plesiosaurio nuevo de Cretáceo del Chubut. Revista del Museo de La Plata (Nueva Serie) 2, 113–130.
Carpenter, K., 1999. Revision of North American elasmosaurs from the Cretaceous of the Western Interior. Paludicola 2, 148–173.
Carpenter, K., Sanders, F., Reed, B., Reed, J., Larson, P., 2010. Plesiosaur swimming as interpreted from skeletal analysis and experimental results. Transactions of the Kansas Academy of Science 113, 1–34.
Chatterjee, S., 2000. The morphology and systematics of *Polarornis*, a Cretaceous loon (Aves: Gaviidae) from Antarctica. In: Proceedings of the 5th Symposium of the Society of Avian Paleontology and Evolution, Beijing, vol. 1, pp. 125–155.
Chatterjee, S., Small, B.J., 1989. New plesiosaurs from the Upper Cretaceous of Antarctica. Geological Society, London, Special Publications 47, 197–215.
Cione, A.L., Medina, F.A., 1987. A record of *Notidanodon pectinatus* (Chondrichthyes, Hexanchiformes) in the Upper Cretaceous of the Antarctic Peninsula. Mesozoic Research 1, 79–88.
Cione, A.L., Santillana, S., Gouiric-Cavalli, S., Hospitaleche, C.A., Gelfo, J.N., López, G.M., Reguero, M., 2018. Before and after the K/Pg extinction in West Antarctica: New marine fish records from Marambio (Seymour) Island. Cretaceous Research 85, 250–265.
Cope, E.D., 1869. Synopsis of the extinct Batrachia, Reptilia and Aves of North America. Transactions of the American Philosophical Society (new series) 14, 1–252.
Crame, J.A., Francis, J.E., Cantrill, D.J., Pirrie, D., 2004. Maastrichtian stratigraphy of Antarctica. Cretaceous Research 25, 411–423.
Cruickshank, A.R.I., Fordyce, R.E., 2002. A new marine reptile (Sauropterygia) from New Zealand: further evidence for a Late Cretaceous Austral radiations of cryptoclidid plesiosaur. Palaeontology 45, 557–575.
de Blainville, H.D., 1835. Description de quelques espèces de reptiles de la Californie, precédée de l'analyse d'un système général d'herpetologie et d'amphibiologie. Nouvelles Archives du Museum d'Histoire Naturelle 4, 233–296.
Dingle, R.V., Lavelle, M., 1998. Late Cretaceous–Cenozoic climatic variations of the northern Antarctic Peninsula: new geochemical evidence and review. Palaeogeography, Palaeoclimatology, Palaeoecology 141, 215–232.
Ditchfield, P.W., Marshall, J.D., Pirrie, D., 1994. High latitude palaeotemperature variation: new data from the Thithonian to Eocene of James Ross Island, Antarctica. Palaeogeography, Palaeoclimatology, Palaeoecology 107, 79–101.
Everhart, M.J., 2000. Gastroliths associated with plesiosaur remains in the Sharon Springs Member of the Pierre Shale (Late Cretaceous), Western Kansas. Transactions of the Kansas Academy of Science 103, 58–69.
Feldmann, R.M., Tshudy, D.M., Thomson, M.R., 1993. Late Cretaceous and Paleocene decapod crustaceans from James Ross Basin, Antarctic Peninsula. Memoir (The Paleontological Society) 28, 1–41.
Fernández, M.S., Gasparini, Z., 2012. Campanian and Maastrichtian mosasaurs from Antarctic Peninsula and Patagonia, Argentina. Bulletin de la Société Géologique de France 183, 93–102.
Friedrich, O., Herrle, J.O., Cooper, M.J., Erbacher, J., Wilson, P.A., Hemleben, C., 2009. The early Maastrichtian carbon cycle perturbation and cooling event: Implications from the South Atlantic Ocean. Paleoceanography 24, PA221 doi:1012/2008PA001654.
Gasparini, Z., Salgado, L., 2000. Elasmosáuridos (Plesiosauria) del Cretácico Tardío del norte de Patagonia. Revista Española de Paleontología 15, 13–21.
Gasparini, Z., Bardet, N., Martin, J.E., Fernández, M., 2003. The elasmosaurid plesiosaur Aristonectes Cabrera from the Latest Cretaceous of South America and Antarctica. Journal of Vertebrate Paleontology 23, 104–115.
Hammer, Ø., Harper, D.A.T., Ryan, P.D., 2001. PAST: Paleontological Statistics Software Package for Education and Data Analysis. Palaeontologia Electronica 4, 1–9.
Henderson, D.M., 2006. Floating point: a computational study of buoyancy, equilibrium, and gastroliths in plesiosaurs. Lethaia 39, 227–244.
Hiller, N., Mannering, A.A., Craig, M.J., Cruickshank, A.R.I., 2005. The nature of *Mauiasaurus haasti* Hector, 1874 (Reptilia: Plesiosauria). Journal of Vertebrate Paleontology 25, 588–601.
Hiller, N., O'Gorman, J.P., Otero, R.A., Mannering, A.A., 2017. A reappraisal of the Late Cretaceous Weddellian plesiosaur genus *Mauisaurus* Hector, 1874. New Zealand Journal of Geology and Geophysics 60, 112–128.
Huber, B.T., Watkins, D.K., 1992. Biogeography of Campanian-Maastrichtian Calcareous Plankton in the region of the Southern Ocean: Paleogeographic and Paleoclimatic Implications. The Antarctic Paleoenvironment: A Perspective on Global Change: Part One 56, 31–60.
Huber, B.T., Norris, R.D., MacLeod, K.G., 2002. Deep-sea paleotemperature record of extreme warmth during the Cretaceous. Geology 30, 123–126.
Hospitaleche, C.A., Gelfo, J.N., 2015. New Antarctic findings of Upper Cretaceous and lower Eocene loons (Aves: Gaviiformes). In: Annales de Paléontologie, 101, pp. 315–324.
Ketchum, H.F., Benson, R.B., 2010. Global interrelationships of Plesiosauria (Reptilia, Sauropterygia) and the pivotal role of taxon sampling in determining the outcome of phylogenetic analyses. Biological Reviews 85, 361–392.
Kriwet, J., Lirio, J.M., Nuñez, H.J., Puceat, E., Lécuyer, C., 2006. Late Cretaceous Antarctic fish diversity. Geological Society, London, Special Publications 258, 83–100.
Kubo, T., Mitchell, M.T., Henderson, D.M., 2012. *Albertonectes vanderveldei*, a new elasmosaur (Reptilia, Sauropterygia) from the Upper Cretaceous of Alberta. Journal of Vertebrate Paleontology 32, 557–572.
Macellari, C.E., 1988. Stratigraphy, sedimentology, and paleoecology of Upper Cretaceous/Paleocene shelf-deltaic sediments of Seymour Island. Geological Society of America (Memoir) 169, 25–54.
Martin, J.E., Crame, J.A., 2006. Palaeobiological significance of high-latitude Late Cretaceous vertebrate fossils from the James Ross Basin, Antarctica. Geological Society, London, Special Publications 258, 109–124.
McArthur, J.M., Crame, J.A., Thirlwall, M.F., 2000. Definition of Late Cretaceous stages boundaries in Antarctica using strontium isotope stratigraphy. The Journal of Geology 108, 623–640.
Montes, M., Nozal, F., Santillana, S., Marenssi, S., Olivero, E., 2013. Mapa Geologico de la isla Marambio (Seymour) Escala 1:20.000 Primera Edicion. Serie Cartografica Geocientıfica Antartica. Madrid-Instituto Geologico y Minero de Espa na; Buenos Aires-Instituto ~ Antartico Argentino.
Noè, L.F., Taylor, M.A., Gómez-Pérez, M., 2017. An integrated approach to understanding the role of the long neck in plesiosaurs. Acta Palaeontologica Polonica 62, 137–162.
Odin, G.S., Matter, A., 1981. De glauconiarum origine. Sedimentology 28, 611–641.
O'Gorman, J.P., 2012. The oldest elasmosaurs (Sauropterygia, Plesiosauria) from Antarctica, Santa Marta Formation (upper Coniacian? Santonian–upper Campanian) and Snow Hill Island Formation (upper Campanian–lower Maastrichtian), James Ross Island. Polar Research 31, 1–10.
O'Gorman, J.P., 2013. Plesiosaurios del Cretácico Superior de Patagoni y Península Antártica, Tomos I y II. PhD thesis. Facultad de Ciencias Naturales y Museo, Universidad Nacional de La Plata, Argentina, p. 527. Unpublished).
O'Gorman, J.P., 2016a. A small body sized Non-Aristonectine Elasmosaurid (Sauropterygia, Plesiosauria) from the late Cretaceous of Patagonia with comments

on the relationships of the Patagonian and Antarctic Elasmosaurids. Ameghiniana 53, 245–268.
O'Gorman, J.P., 2016b. New Insights on the *Aristonectes parvidens* (Plesiosauria, Elasmosauridae) Holotype: news on an old specimen. Ameghiniana 53, 397–417.
O'Gorman, J.P., Coria, R.A., 2017. A new elasmosaurid specimen from the upper Maastrichtian of Antarctica: new evidence of a monophyletic group of Weddellian elasmosaurids. Alcheringa: An Australasian Journal of Palaeontology 41, 240–249.
O'Gorman, J.P., Talevi, M., Fernández, M.S., 2016. Osteology of a perinatal aristonectine (Plesiosauria; Elasmosauridae). Antarctic Science 29, 61–72.
O'Gorman, J.P., Gasparini, Z., Salgado, L., 2013a. Postcranial morphology of *Aristonectes* Cabrera, 1941 (Plesiosauria, Elasmosauridae) from the Upper Cretaceous of Patagonia and Antarctica. Antarctic Science 25, 71–82.
O'Gorman, J.P., Salgado, L., Olivero, E.B., Marenssi, S.A., 2015. *Vegasaurus molyi*, gen. et sp. nov. (Plesiosauria, Elasmosauridae), from the Cape Lamb Member (lower Maastrichtian) of the Snow Hill Island Formation, Vega Island, Antarctica, and Remarks on Wedellian Elasmosauridae. Journal of Vertebrate Paleontology 35, e931285.
O'Gorman, J.P., Salgado, L., Varela, J., Parras, A., 2013b. Elasmosaurs (Sauropterygia, Plesiosauria) from La Colonia Formation (Campanian–Maastrichtian), Argentina. Alcheringa: An Australasian Journal of Palaeontology 37, 259–267.
O'Gorman, J.P., Olivero, E.B., Santillana, S., Everhart, M.J., Reguero, M., 2014. Gastroliths associated with an *Aristonectes* specimen (Plesiosauria, Elasmosauridae), López de Bertodano Formation (upper Maastrichtian) Seymour Island (Is. Marambio), Antarctic Peninsula. Cretaceous Research 50, 228–237.
O'Gorman, J.P., Panzeri, K.M., Fernández, M.S., Santillana, S., Moly, J.J., Reguero, M., 2017. A new elasmosaurid from the upper Maastrichtian López de Bertodano Formation: new data on weddellonectian diversity. Alcheringa: An Australasian Journal of Palaeontology 42, 575–586.
O'Keefe, F.R., 2004. On the cranial anatomy of the polycotylid plesiosaurs, including new material of *Polycotylus latipinnis*, Cope, from Alabama. Journal of Vertebrate Paleontology 24, 326–340.
O'Keefe, F.R., Hiller, N., 2006. Morphologic and Ontogenetic Patterns in Elasmosaur Neck Length, with Comments on the Taxonomic Utility of Neck Length Variables. Paludicola 5, 206–229.
O'Keefe, F.R., Street, H.P., 2009. Osteology of the cryptocleidoid plesiosaur *Tatenectes laramiensis*, with comments on the taxonomic status of the Cimoliasauridae. Journal of Vertebrate Paleontology 29, 48–57.
O'Keefe, F.R., Otero, R.A., Soto-Acuña, S., O'Gorman, J.P., Godfrey, S.J., Chatterjee, S., 2017. Cranial anatomy of *Morturneria seymourensis* from Antarctica, and the evolution of filter feeding in plesiosaurs of the Austral Late Cretaceous. Journal of Vertebrate Paleontology 37, e1347570.
Olivero, E.B., 2012. Sedimentary cycles, ammonite diversity a palaeoenvironmental changes in the Upper Cretaceous Marambio Group, Antarctica. Cretaceous Research 34, 348–366.
Olivero, E.B., Medina, F.A., 2000. Patterns of Late Cretaceous ammonite biogeography in southern high latitudes: the family Kossmaticeratidae in Antarctica. Cretaceous Research 21, 269–279.
Olivero, E.B., Ponce, J.J., Martinioni, D.R., 2008. Sedimentology and architecture of sharp based tidal sandstones in the upper Marambio Group, Maastrichtian of Antarctica. Sedimentary Geology 210, 11–26.
Otero, R.A., 2016. Taxonomic reassessment of *Hydralmosaurus* as *Styxosaurus*: new insights on the elasmosaurid neck evolution throughout the Cretaceous. PeerJ 4, e1777.
Otero, R.A., O'Gorman, J.P., Hiller, N., 2015. Reassessment of the upper Maastrichtian material from Chile referred to *Mauisaurus* Hector, 1874 (Plesiosauroidea: Elasmosauridae) and the taxonomical value of the hemispherical propodial head among austral elasmosaurids. New Zealand Journal of Geology and Geophysics 58, 252–261.
Otero, R.A., Soto-Acuña, S., O'Keefe, F.R., 2018. Osteology of *Aristonectes quiriquinensis* (Elasmosauridae, Aristonectinae) from the upper Maastrichtian of central Chile. Journal of Vertebrate Paleontology 38, e1408638.
Otero, R.A., Soto-Acuña, S., Rubilar-Rogers, D., 2012. A postcranial skeleton of an elasmosaurid plesiosaur from the Maastrichtian of central Chile, with comments on the affinities of Late Cretaceous plesiosauroids from the Weddellian Biogeographic Province. Cretaceous Research 37, 89–99.
Otero, R.A., O'Gorman, J.P., Hiller, N., O'Keefe, F.R., Fordyce, R.E., 2016. *Alexandronectes zealandiensis* gen. et sp. nov., a new aristonectine plesiosaur from the lower Maastrichtian of New Zealand. Journal of Vertebrate Paleontology 36, e1054494.
Otero, R.A., Rubilar-Rogers, D., Yury-Yañez, R.E., Vargas, A.O., Gutstein, C.S., Mourgues, F.A., Robert, E., 2013. A new species of chimaeriform (Chondrichthyes, Holocephali) from the uppermost Cretaceous of the López de Bertodano Formation, Isla Marambio (Seymour Island), Antarctica. Antarctic Science 25, 99–106.
Otero, R.A., Soto-Acuña, S., Vargas, A.O., Rubilar-Rogers, D., Yury-Yáñez, R.E., Gutstein, C.S., 2014a. Additions to the diversity of elasmosaurid plesiosaurs from the Upper Cretaceous of Antarctica. Gondwana Research 26, 772–784.
Otero, R.A., Gutstein, C.S., Vargas, A.O., Rubilar-Rogers, D., Yury-Yáñez, R., Bastías, J., Ramírez, C., 2014b. New chondrichthyans from the Late Cretaceous (Campanian–Maastrichtian) of Seymour and James Ross islands, Antarctica. Journal of Paleontology 88, 411–420.
Otero, R.A., Soto-Acuña, S., O'Keefe, F.R., O'Gorman, J.P., Stinnesbeck, W., Suárez, M.E., Rubilar-Rogers, D., Salazar, C., Quinzio-Sinn, L.A., 2014c. *Aristonectes quiriquinensis*, sp. nov., a new highly derived elasmosaurid from the upper Maastrichtian of central Chile. Journal of Vertebrate Paleontology 34, 100–125.
Owen, R., 1860. On the orders of fossil and recent Reptilia, and theirdistribution in time. Reports of the British Association for the advancement of Science 29, 153–166.
Press, W.H., Teukolsky, S.A., Vetterling, W.T., Flannery, B.P., 1992. Numerical Recipes. Cambridge Univ. Press, New York, p. 994.
Rich, T., Vickers-Rich, P., Fernández, M., Santillana, S., 1999. A probable hadrosaur from Seymour Island, Antarctic Peninsula. National Science Museum Monographs 15, 219–222.
Sachs, S., Kear, B., 2015. Postcranium of the paradigm elasmosaurid plesiosaurian Libonectes morgani (Welles, 1949). Geological Magazine 152, 694–710.
Sachs, S., Kear, B.P., 2017. Redescription of the elasmosaurid plesiosaurian *Libonectes atlasense* from the Upper Cretaceous of Morocco. Cretaceous Research 74, 205–222.
Sachs, S., Hornung, J.J., Kear, B.P., 2017. A new basal elasmosaurid (Sauropterygia: Plesiosauria) from the Lower Cretaceous of Germany. Journal of Vertebrate Paleontology 37, e1301945.
Sachs, S., Lindgren, J., Kear, B.P., 2018. Reassessment of the *Styxosaurus snowii* (Williston, 1890) holotype specimen and its implications for elasmosaurid plesiosaurian interrelationships. Alcheringa: An Australasian Journal of Palaeontology 42, 560–574.
Sanderson, S.L., Wassersug, R., 1993. Convergent and alternative designs for vertebrate suspension feeding. The skull 3, 37–112.
Sato, T., Hasegawa, Y., Manakoto, M., 2006. A new elasmosaurid plesiosaur from the Upper Cretaceous of Fukushima, Japan. Paleontology 49, 467–484.
Serratos, D.J., Druckenmiller, P., Benson, R.B., 2017. A new elasmosaurid (Sauropterygia, Plesiosauria) from the Bearpaw Shale (Late Cretaceous, Maastrichtian) of Montana demonstrates multiple evolutionary reductions of neck length within Elasmosauridae. Journal of Vertebrate Paleontology 37, e1278608.
Tobin, T.S., Ward, P.D., Steig, E.J., Olivero, E.B., Hilburn, I.A., Mitchell, R.N., Diamond, M.R., Raub, T.D., Kirschvink, J.L., 2012. Extinction patterns, δ^{18}O trends, and magnetostratigraphy from a southern high-latitude Cretaceous–Paleogene section: Links with Deccan volcanism. Palaeogeography, Palaeoclimatology, Palaeoecology 350, 180–188.
Vincent, P., Bardet, N., Suberbiola, X.P., Bouya, B., Amaghzaz, M., Meslouh, S., 2011. *Zarafasaura oceanis*, a new elasmosaurid (Reptilia: Sauropterygia) from the Maastrichtian Phosphates of Morocco and the palaeobiogeography of latest Cretaceous plesiosaurs. Gondwana Research 19, 1062–1073.
Welles, S.P., 1943. Elasmosaurid plesiosaurs with description of new material from California and Colorado, vol. 13. Memoirs of the University of California, pp. 125–254.
Welles, S.P., 1952. A review of the North American Cretaceous elasmosaurs, vol. 29. University of California Publications in Geological Sciences, pp. 46–144.
Welles, S.P., 1962. s. In: A new species of elasmosaur from the Aptian of Columbia and a review of the Cretaceous plesiosaur, vol. 44. University of California, Publications in the Geological Sciences, pp. 1–96.
Zinsmeister, W.J., 1979. Biogeographic significance of the late Mesozoic and early Tertiary molluscan faunas of Seymour Island (Antarctic Peninsula) to the final breakup of Gondwanaland. Ohio State University, Institute of Polar Studies, 349–355. In: Gray, J., Boucot, A. (Eds.), Historical Biogeography, Plate Tectonics and the Changing Environment. Proceedings of the 37th Annual Biology Colloquium and Selected Papers. Oregon State University Press, Corvallis.
Zinsmeister, W.J., Feldmann, R.M., Woodburne, M.O., Elliot, D.H., 1989. Latest Cretaceous/earliest Tertiary transition on Seymour Island, Antarctica. Journal of Paleontology 63, 731–738.

Appendix A. Supplementary data

Supplementary data to this article can be found online at https://doi.org/10.1016/j.cretres.2019.05.004.